

FATA: An efficient optimization method based on geophysics

Ailiang Qi¹, Dong Zhao^{1,*}, Ali Asghar Heidari², Lei Liu³, Yi Chen⁴, Huiling Chen^{4,*}

¹ College of Computer Science and Technology, Changchun Normal University, Changchun, Jilin 130032, China
(q17853118231@163.com, zd-hy@163.com)

² School of Surveying and Geospatial Engineering, College of Engineering, University of Tehran, Tehran, Iran
(as_heidari@ut.ac.ir)

³ College of Computer Science, Sichuan University, Chengdu, Sichuan 610065, China
(liulei.cx@gmail.com)

⁴ Key Laboratory of Intelligent Informatics for Safety & Emergency of Zhejiang Province, Wenzhou University, Wenzhou 325035, China
(kenyoncy2016@gmail.com, chenhuilongjlu@gmail.com)

*Corresponding Author: Dong Zhao, Huiling Chen

E-mail: zd-hy@163.com (Dong Zhao), chenhuilongjlu@gmail.com (Huiling Chen)

Abstract

An efficient swarm intelligence algorithm is proposed to solve continuous multi-type optimization problems, named the fata morgana algorithm (FATA). By mimicking the process of mirage formation, FATA designs the mirage light filtering principle (MLF) and the light propagation strategy (LPS), respectively. The MLF strategy, combined with the definite integration principle, drives the algorithmic population to enhance FATA's exploration capability. The LPS strategy, combined with the trigonometric principle, drives the algorithmic individual to improve the algorithm's convergence speed and exploitation capability. These two search strategies can better use FATA's population and individual search capabilities. The FATA is compared with a broad array of competitive optimizers on 23 benchmark functions and IEEE CEC 2014 to verify the optimization capability. This work is designed separately for qualitative analysis, exploration and exploitation competence analysis, the analysis of avoiding locally optimal solutions, and comprehensive comparison experiments. The experimental results demonstrate the comprehensiveness and competitiveness of FATA for solving multi-type functions. Meanwhile, FATA is applied to three practical engineering optimization problems to evaluate its performance. Then, the algorithm obtains better results than its counterparts in engineering problems. According to the results, FATA has excellent potential to be used as an efficient computer-aided tool for dealing with practical optimization tasks. Source codes and related files are available at <https://aliasgharheidari.com/FATA.html> and other websites.

Keywords: Fata morgana algorithm; The mirage light filtering principle; Light propagation strategy; Swarm intelligence algorithm; Engineering optimization

1 Introduction

Optimization methods have been intensely studied in recent years in various domains of real-world problems [1]. Regardless of whether the operations of these methods can be traditional and deterministic or stochastic, their type can fit in one of the single-objective, multi-objective [2], and many objective groups, depending on the number of cost functions to be handled [3]. As one of the leading groups, evolutionary methods have revolutionized how they deal with problems because they use adaptation and self-organization concepts, do not need gradient info [4], and can scan the surface of multi-modal feature spaces [5]. As optimization problems become more complex and multi-type, the need for efficient and accurate optimization methods is growing [6]. Therefore, in the last decade, scholars have studied optimization methods such as linear programming, dynamic programming, machine learning, and swarm intelligence. Various types of methods have been widely used for optimization tasks. Liu et al. [7] proposed a self-adaptive step length estimation model that combines the gradient descent algorithm and the track estimation algorithm to estimate the person's position. Liu et al. [8] presented an exponentially weighted moving average control chart to optimize quality control in asphalt mixture production. Han et al. [9] proposed a novel decay function to determine the accuracy requirement of the convolutional neural network model. Tu et al. [10] introduced a novel version of the whale optimization algorithm combined with a communication mechanism for the optimal design of engineering problems. Many traditional optimization methods that rely on gradient information have poor convergence [11]. These are difficult-to-handle multi-type problems [12] and continuous problems. In recent years, swarm intelligence algorithms (SIAs) with better robustness and optimization capability have effectively compensated for these shortcomings [13].

Moreover, swarm intelligence algorithms have a natural advantage when dealing with high-dimensional, big data, and non-differentiable tasks. Meanwhile, SIA features black-box calculations and a simpler solution process. In Figure 1, the SIA derives many algorithms, including swarm-based, evolutionary, human, and physics-based algorithms.

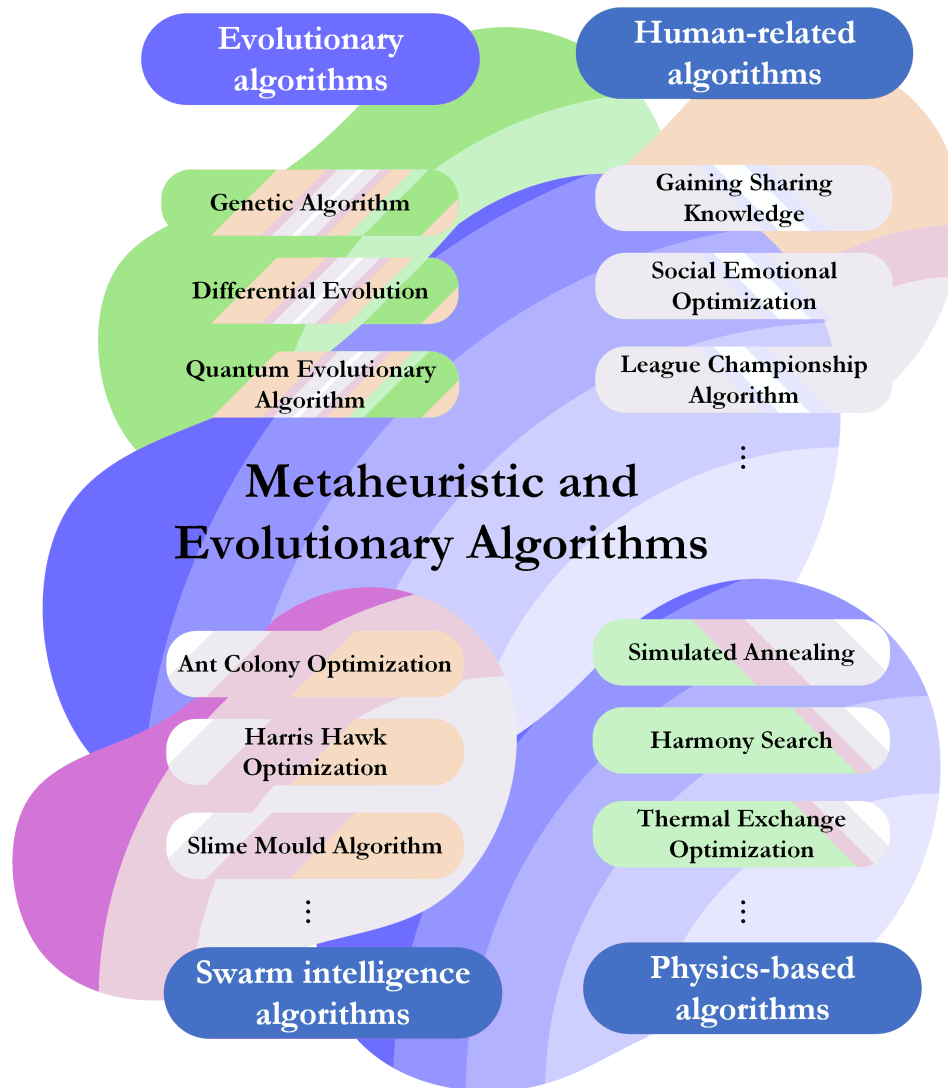


Figure 1. The classification of SIAs

(1) **Swarm-based algorithm.** In 1991, Dorigo et al. proposed an ant colony optimization algorithm inspired by the foraging behavior of ant colonies to solve discrete problems. To further solve the continuous problems, the ant colony optimization algorithm (ACOR) has been improved [14]. Despite the clever design of ACOR's core strategy, the algorithm's ability to search for optimal values is not good enough. In 1995, Kennedy et al. [15] proposed a particle swarm algorithm (PSO) inspired by bird flocks' predatory behavior. However, the convergence speed of the algorithm is slow. Therefore, many variants of PSO have been proposed over the years [16]. Lynn et al. [17] proposed an enhanced PSO (EPSO) based on the ensemble strategy to solve parameter optimization tasks. Issa et al. [18] presented a novel PSO variant by merging it with the sine cosine algorithm named ASCA_PSO. The proposed method performs well in solving optimal solutions and computing time. The moth-flame optimization (MFO) [19] has excellent exploitation capability. Meanwhile, some improved algorithms for MFO have been developed in recent years. An improved MFO (DSMFO) was presented, combining the sine-cosine and differential evolution mechanisms to enhance the

balance [20]. In 2020, Li et al. [21] proposed a new algorithm that combines the adaptive weights strategy with a unique mathematical function, named the slime mould algorithm (SMA). As researchers delve deeper into the swarm-based algorithm, more and more algorithms have been proposed, such as Harris Hawks optimization (HHO) [22], crow search algorithm (CSA) [23], bat-inspired algorithm (BA) [24], colony predation algorithm (CPA) [25], hunger games search (HGS) [26], parrot optimizer (PO) [27], liver cancer algorithm (LCA) [28], and firefly algorithm (FA) [29].

Then, the grey wolf optimizer (GWO) [30], whale optimization algorithm (WOA) [31], and fruit fly optimization algorithm (FOA) [32] were developed. These algorithms are very active SIAs. So, some improved variants have been proposed, especially for GWO [33]. Zhu et al. [34] introduced an enhanced GWO named HGWO to enhance the diversity of its populations. Elhosseini et al. [35] proposed a version of the WOA that combined the inertia weight strategy and the non-linear parameter strategy. Li et al. [36] proposed a new type of WOA based on decomposition, which combined with the decomposition framework based on penalty-Tchebycheff value to overcome the shortcomings of premature in the complex search space and applied it to the optimization of aeroengine turbine disk structures. Wang et al. [37] introduced an adaptive mutation FOA (AMFOA), which enhanced the convergence speed of the original algorithm. Hu et al. [38] proposed a new variant of FOA by using the decreasing step size strategy to improve the algorithm's performance.

(2) Evolutionary algorithm. Darwin's theory of evolution inspired evolutionary algorithms. In 1997, the classical differential evolution algorithm (DE) was proposed by Storn et al. [39]. DE has the disadvantage of quickly falling into the local optimum. So many variants of the algorithm combining other methods have been proposed. For example, Nenavath designed a hybridizing DE algorithm with a sine cosine strategy [30]. Qin et al. [40] proposed a new DE (SADE) variant with a self-adaptive strategy. Moreover, many other evolutionary algorithms have also been proposed, such as the genetic algorithm (GA) [41]. Among them, the search strategies of GA were designed based on gene selection, crossover, and mutation. Because of its solid theoretical foundation, GA and its improved variants were widely used in various scientific fields [42]. Li et al. [43] proposed a novel genetic algorithm with adaptive selection using non-inductive transfer learning to solve dynamic optimization problems. Also, the paper [44] proposes a dynamic genetic optimization algorithm based on a hierarchical response system that mainly integrates diversity, memory, and prediction methods to respond flexibly to environmental changes.

(3) Human-based algorithm. The history of human evolution inspired human-based algorithms. Meanwhile, many other human-based algorithms have also been proposed, such as teaching-learning-based optimization (TLBO) [45], tabu search (TS) [46], weighted mean of vectors (INFO) [47], and Runge Kutta optimization algorithm (RUN) [48]. The algorithm has comprehensive optimization performance and high algorithmic complexity.

(4) Physics-based algorithm. Just as nature is all-encompassing, physics-based algorithms have

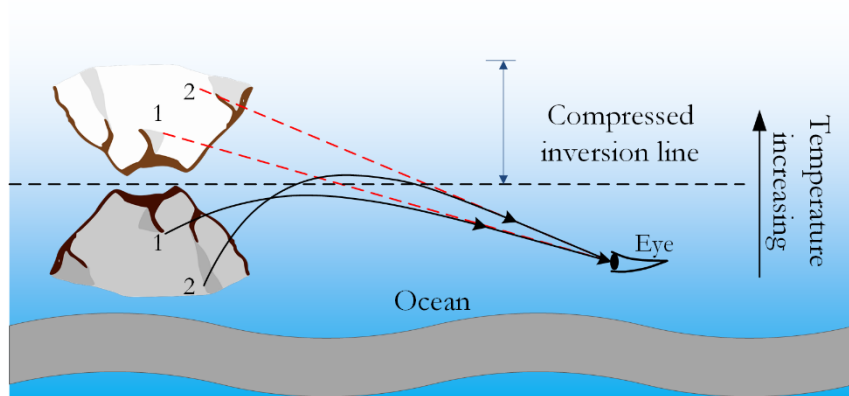
evolved rapidly in recent years, such as the simulated annealing (SA) and its variants [49], multi-verse optimizer (MVO) and its variants [50], and the gravitational search algorithm (GSA) and its variants [51]. They have been designed based on physical principles and numerical methods, demonstrating excellent optimization capabilities.

In addition, Shah-Hosseini et al. [52] proposed the intelligent water drops algorithm (IWD) inspired by the water cycle system in nature in 2007. In 2016, the sine cosine algorithm (SCA) combining trigonometric formulas [53] was proposed. Subsequently, many other variants of the SCA have been developed. Qu et al. [38] proposed a modified SCA (m_SCA), which combined the neighborhood search mechanism and the greedy levy mutation strategy to improve its convergence speed. A novel variant of the SCA [54] was presented, combining the Cauchy and Gaussian strategies. In 2022, the poplar optimization algorithm (POA) [55] was proposed to mimic the sexual and asexual propagation mechanisms of poplar for numerical optimization and image segmentation.

The above algorithms play an essential role in optimization but also have limitations. Some algorithms have disadvantages in the design of parameters, complexity, and computational cost. The individual search strategy of many algorithms is the same as the population search strategy, which seriously affects the balance between global exploration and local exploitation. That also leads to the inefficiency of the algorithm in solving multi-type continuous optimization problems. Based on the above problems, a physics-based fata morgana algorithm (FATA) inspired by the process of mirage formation is proposed to improve the optimization efficiency. Due to the uneven density of the air caused by light, a unique mirage landscape can form at sea level, as shown in Figure 2a. Figure 2b illustrates the mirage phenomenon in nature. In the Figure 2b, the increasing temperature causes the air to become an inhomogeneous density medium. An observer looking through the inversion line can see the phenomenon of a compressed mirage.



(a)



(b)

Figure 2. Mirage phenomenon based on work in [56]

FATA constructs two strategies for population search and individual search through the principle of the mirage phenomenon, thus solving the optimization problem. (1) FATA designs the mirage light filtering principle as the population search strategy of the algorithm, which combines the principle of definite integration. (2) FATA designs three light propagation strategies (refraction, refraction, and total internal reflection) as individual search strategies for the algorithm. Therefore, the population is adaptive to perform local exploitation and avoid the local optimum (LO). The following experiments are utilized to verify the performance of FATA. (1) The multi-performance of FATA on function sets has been verified, including exploration ability, exploitation ability, the analysis of avoiding locally optimal solutions, and the comprehensive algorithm. (2) The comparison experiments between FATA and its original and improved counterparts are designed to verify the comprehension of the algorithm. This work evaluates the experimental results using a variety of analytical methods, including the Wilcoxon signed-rank test (WSRT) [57], the Friedman test (FT) [58], the average (AVG), the standard deviation (STD), etc. The following four points are the innovations and contributions of this work.

- A novel swarm intelligence algorithm called FATA was first proposed.
- The mirage light filtering principle and the light propagation strategy are employed to improve the competitiveness of FATA. The former is combined with the definite integral principle for population search, while the latter is combined with the trigonometric principle for individual search.
- To fully demonstrate the advantages of the proposed algorithm on multi-type function sets, the FATA is compared with other excellent algorithms on benchmark function sets.
- The proposed FATA is applied to optimize three engineering design problems, including welded beam design, pressure vessel design, and cantilever structure design.

The paper structure of the study is partially as follows: Section 2 introduces the concepts and inspiration of the mirage. In Section 3, the principle of the Fata morgana algorithm is described in detail, and the structure of the FATA is introduced. This work shows the experimental results of

FATA in benchmark functions in Section 4 and analyzes the performance and characteristics of the algorithm. In Section 5, the experimental results of the FATA application to engineering problems are analyzed and presented. Sections 6 and 7 discuss and summarize the main work of this paper and present future work.

2 Inspiration for the fata morgana phenomenon

The fata morgana (mirage) is a common physical phenomenon in nature. The mirage phenomenon formed by light propagation is the reflection of light from an object into an atmosphere of uneven density (from an optically denser medium to an optical thinning medium). By analyzing the phenomenon of mirages formed by the propagation of light rays emitted from underwater hills, this paper proposes the design of Figure 3, illustrating the optical propagation process of light rays emitted from a ship in the ocean that forms a mirage. Forming a mirage requires both an inhomogeneous density medium and light propagation in this medium. First, the atmospheric temperature will change because of the sunlight to form the inhomogeneous density medium. At this moment, the light reflected by the boat into this medium, the light in the propagation process, constantly changes the refraction angle, and eventually, the phenomenon of total internal reflection, the formation of the mirage. The mirage can be seen when the observer (Eye in Figure 3) looks at the sky in a red direction.

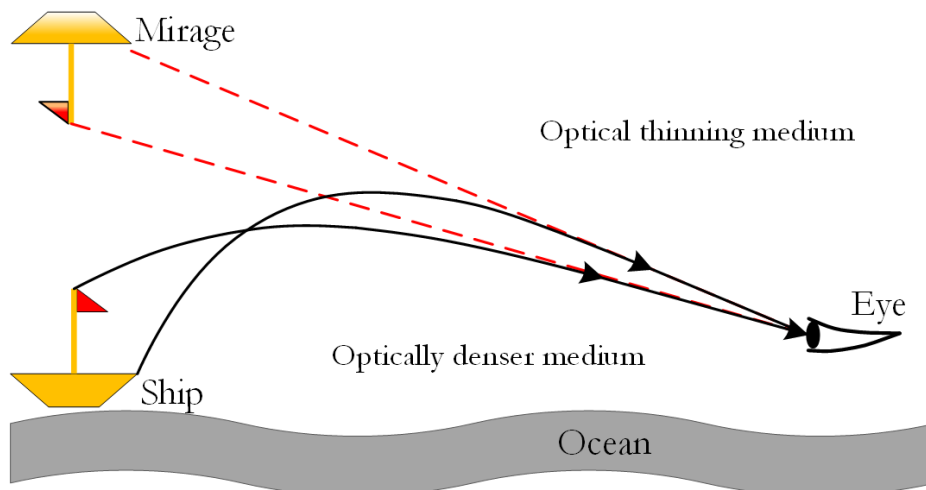


Figure 3. The formation of the mirage

According to the entire process of mirage phenomenon formation depicted in Figure 3, the light emitted from the ship's body can only form a mirage if it balances filtering the mirage light and light refraction/reflection operations during the propagation process. As mentioned earlier, there is currently an imbalance in the execution of population global search and individual local search strategies in swarm intelligence algorithms while searching for optimal values. Inspired by the balanced execution of filtering mirage light and light refraction/reflection operations in forming the

mirage phenomenon, algorithms designed based on the mirage principle aim to balance global search and local search strategies during optimization, thereby demonstrating the best optimization capability. Instead of algorithms like the HHO, which simulate the global search and local search strategies of swarm intelligence algorithms using the soft and hard besiege strategies of hawk hunting, execute these strategies sequentially without maintaining a good balance.

Furthermore, based on the mirage principle, Figure 3 provides a detailed analysis of the ability of the algorithm to balance global search and local search strategies through the analysis of mirage light propagation. In the figure, when the object shoots light at the ship, some light will enter the atmosphere of inhomogeneous density. As the light propagates from an optically denser medium to an optically thinning medium in the atmosphere, the refractive index changes continuously to refract the light at an increasing angle. In the optical thinning medium, the light reaches the critical angle and undergoes the phenomenon of total internal reflection. Last, the mirage phenomenon is formed.

Therefore, incorporating the mirage principle into the design of swarm intelligence algorithms, this paper introduces the mirage light filtering principle and the light propagation principle based on the filtering of mirage light formation and the refraction and reflection operations of light, respectively. In the mirage phenomenon, the mirage light filtering principle can select light to form the mirage and filter out other light. The light propagation principle in a medium of inhomogeneous density can constantly change the direction and size of light.

Among them, the population search strategy of FATA (named the mirage light filtering principle) is inspired by the light reflected by the boat into the medium. The principle of light propagation inspires the individual search strategy of FATA (named the light propagation strategy) in the medium with inhomogeneous density. These two strategies are at the core of the FATA (fata morgana algorithm). FATA balances the mirage light filtering principle and the light propagation strategy responsible for global exploration and local algorithm exploitation. Therefore, the mirage formation process is entirely consistent with it, which creates the conditions for the proposed fata morgana algorithm.

3 Fata morgana algorithm

In Figure 4, multiple light that forms a mirage in the fata morgana algorithm is used as the population, while light (\mathbf{x}) is used as the individual. The mirage (\mathbf{x}_{best}) is used as the optimization target.

In the first stage, the multiple light population is dynamically evaluated according to the mirage light filtering principle based on the definite integral principle. The multiple light emitted from the hull in the lower left corner of Figure 4, including the light rays that have undergone physical transformation and formed a mirage (\mathbf{x}_{best}), and the light rays that have undergone physical

transformation and are directed elsewhere without forming a mirage (x_{best}).

In the second stage, the mirage light population executes the light propagation strategy (including the first half, the second half refraction strategy, and the total internal reflection). The physical change of light propagation in a medium with inhomogeneous density is the process of exchanging individual information, and the algorithm searches for the target to produce the mirage (optimal solutions).

3.1 The mirage light filtering principle

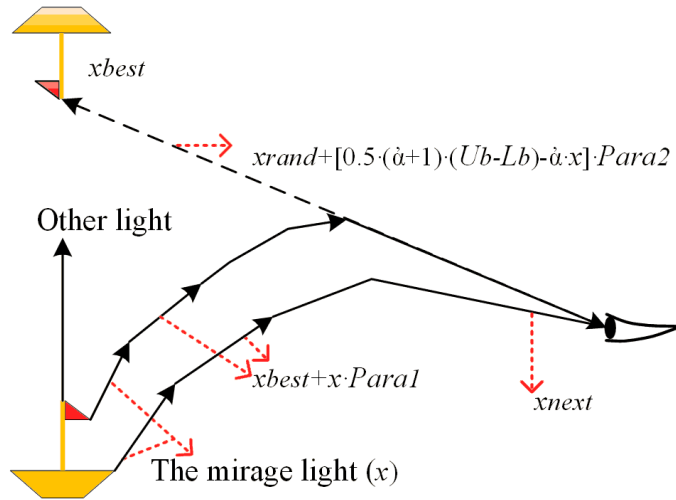


Figure 4. FATA optimization process in 3-dimension

The section shows the Fata Morgana algorithm's population search strategy based on the principle of definite integral. In Figure 4, during the physical process of mirage formation, the hull emits two types of light rays. The majority of the light rays belong to the first type (other light in Figure 4), which do not propagate and form a mirage. The other type of light rays undergoes physical transformations that result in the formation of a mirage and are referred to as the mirage light (x).

In FATA, distinguishing between the two types of light populations is crucial for the algorithm to find x_{best} . Therefore, FATA employs a light population quality evaluation strategy based on the definite integral principle to assess the different types of light populations. In swarm intelligence algorithms, population quality is evaluated by calculating individuals' fitness and then aggregating the fitness values for the entire population. As shown in Figure 5a, if the fitness of individuals in a light population is ranked, it forms a cumulative curve. To efficiently compute the fitness of different types of light populations (other light, the mirage light), FATA utilizes definite integration to evaluate the curve in Figure 5b, using the integral value as a measure of fitness. The mirage light (x) that is selected based on the definite integral principle is also referred to as the filtered mirage light population.

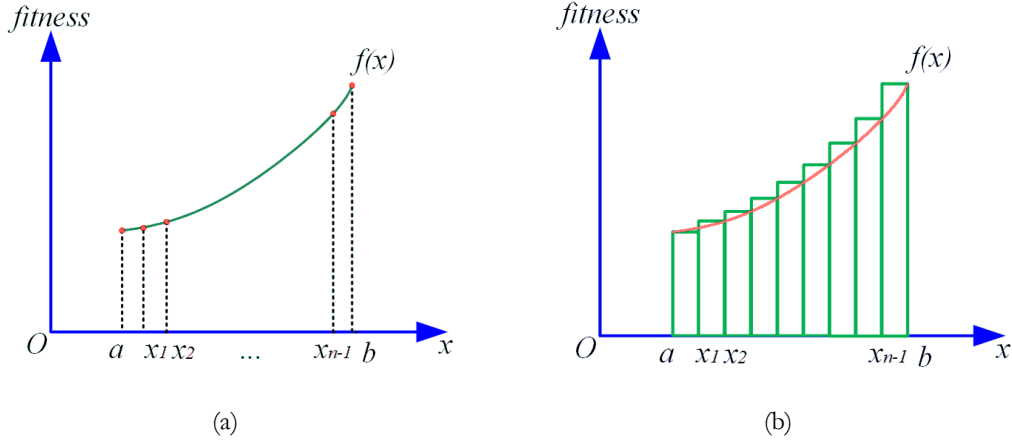


Figure 5. The population fitness curve of FATA

First, the strategy determines the population as other light, or the mirage light based on the population quality to perform different search methods (Eq. (1)). Population quality means the overall quality of the population. In the strategy, the integrated area (S) of the population fitness function ($f(x)$) represents the population quality. Figure 5a shows the population fitness function curve. Figure 5b shows the integrated area (S) of the curve.

Fitness in the SIA represents individual quality. However, discrete and high-dimensional fitness values are difficult to use as an evaluation criterion for the population's overall quality. Therefore, all individual fitness in the population is fitted to a function ($f(x)$). Among them, the fata morgana algorithm is based on the principle of definite integration to calculate the integrated area (S) of the population fitness function curve.

$$x_i^{next} = \begin{cases} L_b + (U_b - L_b) \cdot rand & , rand > P \\ x_{best} + x_i \cdot Para_1 & , rand \leq P \text{ and } rand < q \\ x_{rand} + [0.5 \cdot (\alpha + 1)(U_b - L_b) - \alpha x_i] \cdot Para_2 & , rand \leq P \text{ and } rand \geq q \end{cases} \quad (1)$$

$$P = \frac{S - S_{worst}}{S_{best} - S_{worst}} \quad (2)$$

$$q = \frac{fit_i - fit_{worst}}{fit_{best} - fit_{worst}} \quad (3)$$

x is the light individual. x^{next} is the new individual. Algorithm 1 demonstrates the mirage light filtering principle of the fata morgana algorithm. Among them, Eqs. (2-3) are the first-half refraction strategy, the second-half refraction strategy, and the total internal reflection strategy, respectively (Section 3.2 will introduce them in that order). In Eq. (4), P is the quality factor of the light population. The smaller the value of S , the better the population's quality. S_{worst} represents the quality of the worst population. S_{best} represents the quality of the best population. The mirage light populations have excellent population quality. In Eq. (5), q is the individual quality factor. fit_i represents the fitness of the current individual (x). fit_{worst} represents the fitness of the worst individual. fit_{best} represents the fitness of the best individual.

Algorithm 1 The mirage light filtering strategy

Input: light individual x ;

Fit the population quality function $f(x)$ according to the fitness of the individuals;
 Calculate the integrated area S of the $f(x)$ based on the principle of definite integration;
 Update the optimal area S_{best} and the worst area S_{worst} ;
 Calculate the population quality factor P by Eq. (4);

If $rand > P$

The population is the light rays directed towards a medium with inhomogeneous density populations;

The population performs Eq. (1) to initialize the population randomly;

Else

The population is the light rays not directed towards a medium with inhomogeneous density populations;

The population executes the search strategy (Eqs. (2-3));

End If

Return new individual x^{next} ;

$$y = f(x) = \sum_{j=0}^n c_j \varphi_j x \quad (6)$$

$$S = \int_a^b f(x) dx \approx \frac{b-a}{n} \cdot \left(\frac{y_0 + y_1}{2} + \frac{y_1 + y_2}{2} + \dots + \frac{y_{n-1} + y_n}{2} \right) \quad (7)$$

Eqs. (6-7) show the method of calculating the area of the population fitness curve $f(x)$ ($f(x_1) < f(x_2) \dots < f(x_i) \dots < f(x_n)$) based on the principle of definite integration. The principle of definite integrals uses the idea of the limit to calculate the area (S) of integration of $f(x)$. Eq. (6) is the population quality fitting function $f(x)$ with points on the curve as (x_i, y_i) and $i \in [1, n]$. c_j and φ_j are parameters.

3.2 The light propagation principle

The light propagation principle in FATA is executed after the mirage light filtering principle, and it serves as the individual search strategy of the algorithm responsible for local exploitation in the search space to find local minima. As shown in Figure 6, the light population of FATA, represented by the mirage light rays, starts from the small boat in the lower-left corner. First, it undergoes the mirage light filtering strategy, where the light population is evaluated and filtered based on the principles of calculus to select the individuals that form the mirage phenomenon. Furthermore, the filtered mirage light population undergoes refraction and reflection sequentially. The individual changes in the light population during refraction and reflection can be observed in Figure 6. The light rays change in direction and size during the processes of refraction and reflection shown in the figure. As an individual search strategy, performing local exploitation in the search space to find a local minimum.

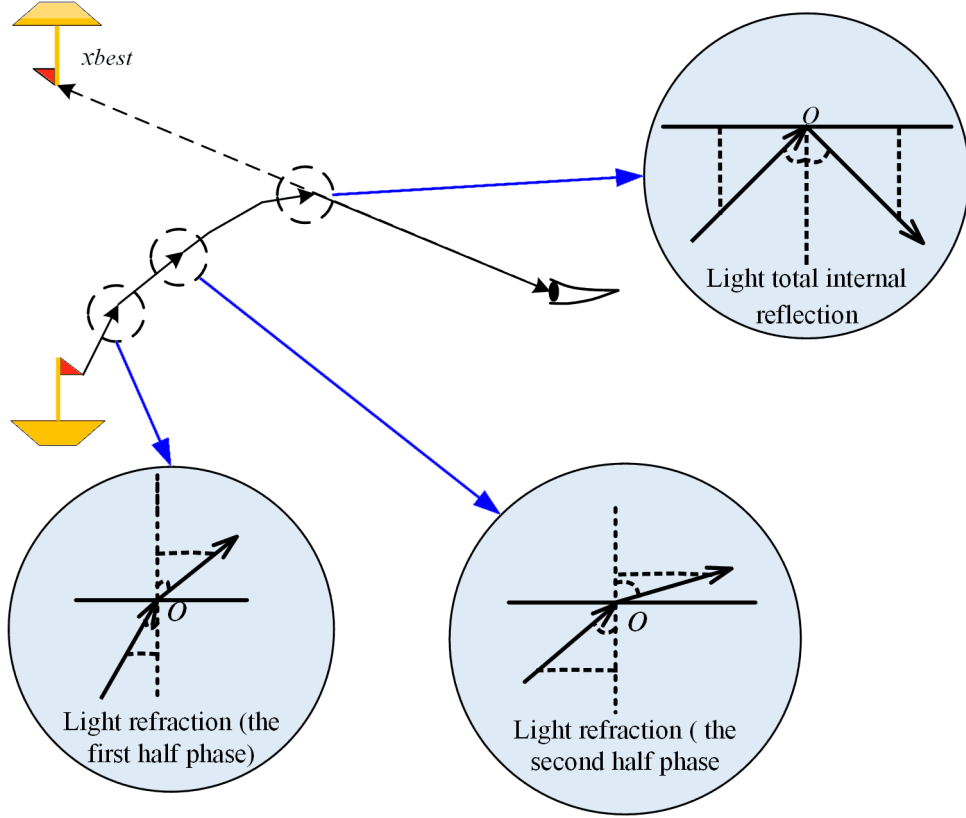


Figure 6. FATA is based on the mirage principle

The fata morgana algorithm designs the individual search strategy based on the light propagation principle combined with trigonometric functions. The algorithm chooses to execute the reflection strategy (the first half phase), the reflection strategy (the second half phase), and the refraction strategy based on the individual quality factor (in Eq. (5)).

Light refraction (the first half phase). In Figure 7, the light x enters the medium with inhomogeneous density in the first half refraction, from optically denser medium to optical thinning medium propagation, changing the direction and size of the light. The angle of incidence (i_1) is smaller than the angle of refraction (i_2).

Figure 7 analyzes the refraction process of the light individual. The light individual is x . $level$ is the surface the refractive surface. In Eq. (8), x^{next} is a new individual after the first half reflection strategy. Assume $NO = C \cdot OM$ where C is a constant. Eqs. (8-10) are the formulas for the strategy.

$$x^{next} = x_{best} + x_z \quad (8)$$

$$x_z = x \cdot Para_1 \quad (9)$$

$$Para_1 = \frac{\sin(i_1)}{C \cdot \cos(i_2)} = \tan(\theta) \quad (10)$$

x^{next} is the new individual. x_{best} is the current best individual. x_z represents the refraction step of the strategy. $Para_1$ is the first-half refraction ratio. $Para_1$ is changing in the process of light propagation. In Eq. (10), to simply measure the incident angle (i_1) and the reflection angle (i_2) during refraction, the parameter θ replaces the angle change in the fata morgana algorithm, $\theta \in [0,1]$.

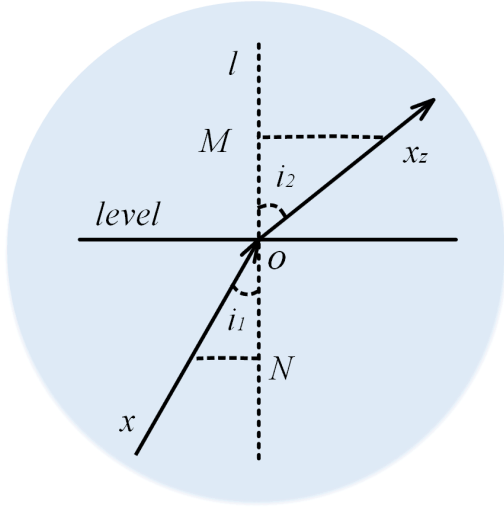


Figure 7. First refraction process of light

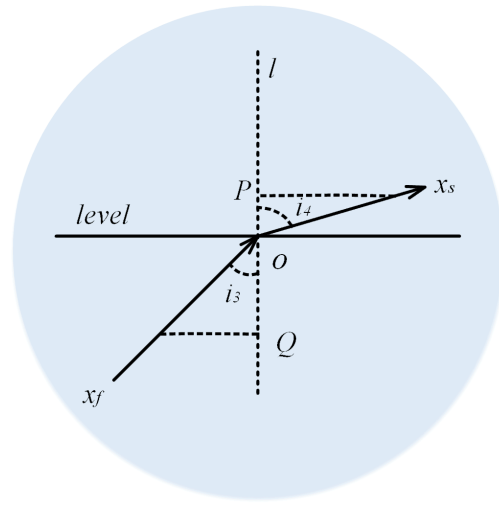


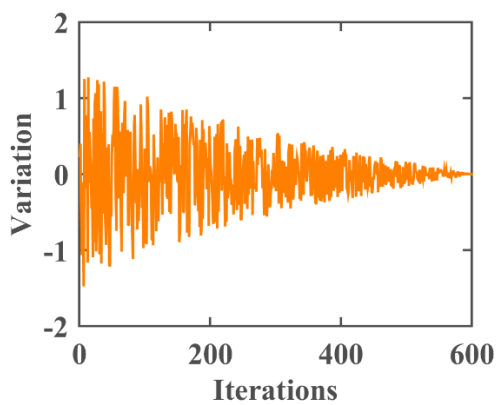
Figure 8. Second refraction process of light

Light refraction (the second half phase). After performing the first half refraction phase, the light performs the second half refraction phase at random points. Figure 8 analyzes the second half refraction process of light. The angle of incidence i_3 is less than the angle of refraction i_4 . The light propagates in a medium with inhomogeneous density, so the refractive index ($Para_2$) changes continuously. In the second half refraction strategy, the light individual (x_f) will generate a new individual (x^{next}) based on random individuals (x_{rand}) in the search space. Eqs. (11-13) are the formulas for the strategy of FATA.

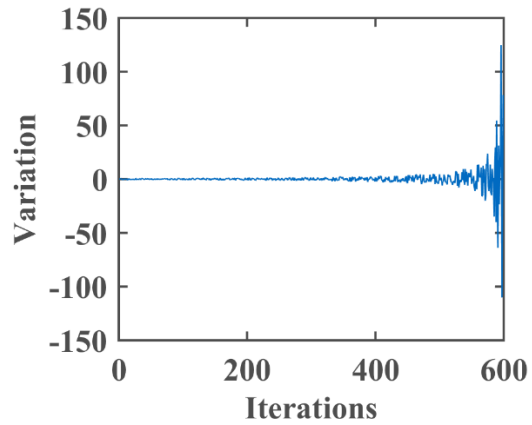
$$x^{next} = x_{rand} + x_s \quad (11)$$

$$x_s = x_f \cdot Para_2 \quad (12)$$

$$Para_2 = \frac{\cos(i_5)}{C \cdot \sin(i_6)} = \frac{1}{\tan(\theta)} \quad (13)$$



(a)



(b)

Figure 9. (a) Trends of $Para_1$ (b) Trends of $Para_2$

x_s is the refraction step in the second half refraction strategy. x_{rand} is a random individual from the population. $Para_2$ is the second refraction ratio. In Figure 9a, the value of $Para_1$

oscillates randomly between $[-2,2]$ and gradually approaches zero as the increment of iterations. In Figure 9b, the value of $Para_2$ oscillates randomly between $[-150,150]$ and gradually increases with the number of iterations. It is found in Figure 9 that the values of the two parameters are relatively large. To standardize $Para_1$ and $Para_2$, they are standardized. The strategy scales the two parameters to the interval $[0,1]$. The substantial oscillation of $Para_2$ at the last phase of the fata morgana algorithm enhances the ability to avoid the local optimum.

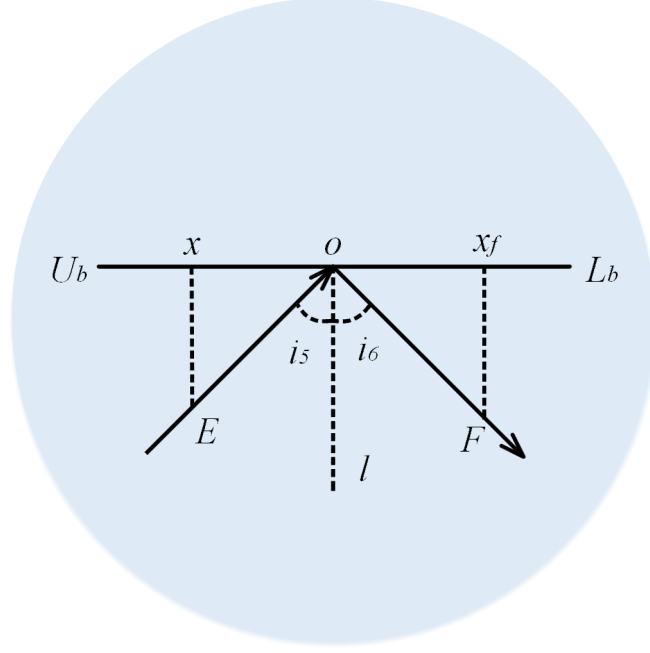


Figure 10. Total reflection process of light

Light total internal reflection. The total internal reflection phase is the final stage of light propagation in the formation of the mirage phenomenon. This is because as the refraction angle increases, the light undergoes total internal reflection in the medium with inhomogeneous density. The total internal reflection strategy drives the FATA population to explore in the opposite direction. Figure 10 analyzes the reflection process of light. The angle of incidence i_5 is equal to the angle of reflection i_6 . In the figure, $O(x_0, 0)$ is the center point of the interval $([L_b, U_b])$. E and F are the distances of the incident and refracted light to the horizontal plane, respectively. In the strategy, the light individual (x) is transformed into the individual (x^{next}) to search for the target in the opposite direction. Eqs. (14-17) are the formulas for the strategy of the fata morgana algorithm.

$$x^{next} = x_f = 0.5 \cdot (\alpha + 1)(U_b + L_b) - \alpha x \quad (14)$$

$$\alpha = \frac{F}{E} \quad (15)$$

$$x_0 - x_f = \frac{F \cdot (x - x_0)}{E} \quad (16)$$

$$x_0 = \frac{U_b - L_b}{2} + L_b = \frac{U_b + L_b}{2} \quad (17)$$

x_f is the reflected individual by the total internal reflection strategy. α is the reflectance of the reflection strategy. α controls the pattern of change in the light individual. When α is greater than 1,

x^{next} crosses the boundary, $\alpha \in [0,1]$. Therefore, the value of α will be discussed in section 4.2. U_b represents the upper limit of the individual position. L_b represents the lower limit of the individual position.

3.3 Algorithm' complexity analysis for FATA

The complexity of the fata morgana algorithm is divided into several parts, including the initialization phase, fitness evaluation phase, sorting phase, and location update phase. First, let's analyze the FATA algorithm's algorithmic time complexity from the data structures perspective. The algorithm parameters are assumed to include population size (n), evaluation number ($MaxFEs$), and dimension (d). Through detailed calculations, the complexity of the initialization phase is $O(n)$. The fitness evaluation and sorting phase complexity are $O(n + n \log n)$. The complexity of the location update is $O(n \cdot d)$. Therefore, the overall complexity of the fata morgana algorithm is $O(n \cdot (1 + MaxFEs (1 + \log n + d)))$. Furthermore, Table 1 presents the algorithmic time complexity of other representative swarm intelligence algorithms, which provides a more intuitive analysis of the algorithmic complexity of FATA. Additionally, the experimental section 4.10 presents the bar charts displaying the computational time statistics of FATA and the comparison algorithms on the function set.

Table 1 The algorithmic time complexity

Algorithm	Complexity($O(c)$)
FATA	$O(n(1 + MaxFEs (1 + \log n + d)))$
MVO	$O(MaxFEs(n^2 + n \cdot d \cdot \log n))$
AOA	$O(n(MaxFEs \cdot L))$; L is number of parameters
ACOR	$O(MaxFEs \cdot n \cdot k \cdot d)$
LCA	$O(n(MaxFEs + MaxFEs \cdot d + 1))$
HHO	$O(n(MaxFEs + MaxFEs \cdot d + 1))$
XMACO	$O(MaxFEs(k + n \cdot (k + d \cdot k + 2d)))$
RIME	$O(MaxFEs(n^2 + n \log n))$

From Table 1, it can be observed that the maximum time complexity of the FATA is $O(MaxFEs \cdot n \log n)$, which is better than the maximum time complexity of algorithms MVO, AOA, and RIME. However, the maximum time complexity of FATA is greater than the time complexities of algorithms ACOR, LCA, HHO, and XMACO, which are $O(MaxFEs \cdot n)$. In the experimental section 4.10, FATA demonstrates expected similarity or lower computational time compared to the MVO, AOA, and RIME algorithms on the function set. Additionally, FATA exhibits lower computational time compared to algorithms such as ACOR, LCA, HHO, and XMACO, showcasing its faster convergence speed and more balanced global and local search capabilities based on the mirage light filtering principle and the light propagation principle inherent in FATA.

To further observe and analyze the algorithmic structure of FATA, the pseudocode of the entire FATA can be presented in Algorithm 2. Additionally, Figure 11 depicts the flowchart of the FATA, illustrating the optimization process of the two main population updating strategies in the FATA. The algorithmic structure of FATA mainly consists of population initialization, parameter initialization, and an iterative loop structure for the evolution strategy. Within the loop structure, the time complexity of the mirage light filtering principle and the light refraction strategy is primarily dependent on the number of iterations and is $O(n(\text{MaxFES} \cdot d))$.

Algorithm 2 Pseudocode of fata morgana algorithm

Input: parameters n , d , MaxFES ;

Output: best Individual;

Initialization parameters Para_1 , Para_2 , α ;

Initialize a population x of size n ;

Calculate the fitness of each individual;

While ($\text{FES} \leq \text{MaxFES}$)

 update *best fitness*, x_{best} ;

 Calculate weights P by Eq. (4);

 Calculate Para_1 and Para_2 by Eq. (10) and Eq. (17);

For $i = 1 : n$

 Execute Algorithm 1 to realize **the mirage light filtering principle**;

If $\text{and} > P$

 the light population performs Eq. (1) to initialize the population randomly;

Else

If $\text{rand} < q$

 Update the individual x_i by Eq. (8) according to **the first half light refraction strategy**;

Else

 Update the individual x_i by Eq. (11) according to **the second half light refraction strategy**;

 Update the individual x_i by Eq. (14) according to **the light total internal reflection strategy**;

End If

End If

End For

$t = t + 1$;

End While

Return the best individual x_{best} ;

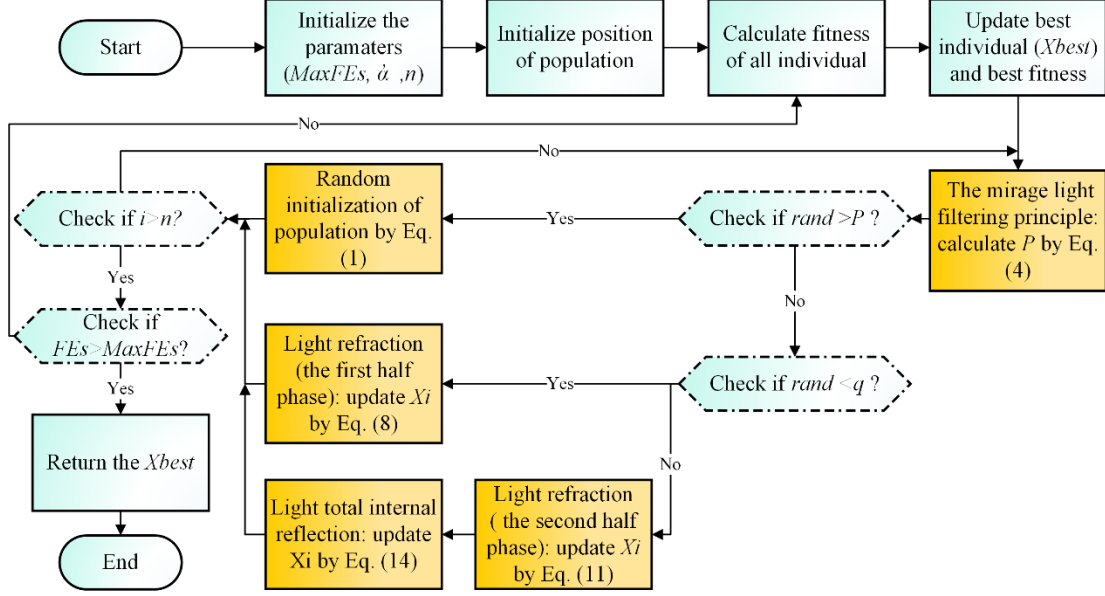


Figure 11. The flowchart of the fata morgana algorithm

4 Experimental results and analysis

Benchmark datasets are widely accepted tools utilized for evaluating the performance of various algorithms. In this section, benchmark function experiments are designed to test the performance of the FATA on multi-type function sets. (1) Reflectance analysis experiments in FATA are designed. The results of the experiments determined the value of reflectance. (2) The qualitative analysis experiments are designed to show the search trend of the light population of the FATA. (3) The FATA is compared with other comparative algorithms to verify the local exploitation capability global exploration capability. (4) The FATA algorithm was compared to state-of-the-art algorithms to demonstrate its efficiency and excellence. Additionally, the experimental results include computational cost statistics for all the algorithms involved.

The algorithms compared in the experiments include the physics-based algorithm (MVO [50], SCA [53], AOA [59], GSA [51]), the swarm-based algorithm (ACOR [14], PSO [15], WOA [31], CSA [23]), the excellent improved algorithm (ACWOA [35], m_SCA [60], HGWO [34], CGSCA [54], AMFOA [37], DSMFO [20], SFOA [38]), the PSO-improved algorithm (EPSO [17], ASCA_PSO [18]), the DE-improved algorithm (SCADE [61], SADE [40]), the 2017 CEC winners (MPEDE [62], LSHADE), rime optimization algorithm (RIME) [63], LCA [28], Harris hawks optimization (HHO) [64] and XMACO [65]).

The experimental results are evaluated by the Wilcoxon signed-rank test (WSRT) [57], the Friedman test (FT) [58], the mean, and the standard deviation, which verified the excellent performance of FATA on different function types. Table 2 shows the parameter settings of the original counterparts.

Table 2 Parameter setting of the model in the experiment

The value of the parameter	
MVO	Existence probability $\in [0.2, 1]$; traveling distance rate $\in [0.6, 1]$
SCA	$A = 2$
WOA	$a_1 = [2, 0]$; $a_2 = [-2, -1]$; $b = 1$
AOA	$\alpha = 5$; $\mu = 0.5$
DE	crossover probability=0.5; Scaling factor=0.5
CSA	$AP = 0.1$; $fl = 2$
GSA	$G_0 = 100$; $\alpha = 20$
PSO	$c_1 = 2$; $c_2 = 2$
ACOR	$k = 10$; $\xi = 1$; $q = 0.5$

All trials are tested under identical circumstances to guarantee the experiments' fairness. The values of each parameter in the experiment are set to population size (30), dimension (30), and evaluation number (300,000). All experiments' algorithms employ evaluation principles (FEs) to restrict the number of algorithm calculations. The evaluation concept guarantees our experiments' reliability and validity. Additionally, the tests are carried out with the following settings to provide a consistent environment for all of them:

- OS: Windows Server, Windows 10 pro
- CPU: AMD Ryzen 9 3900x 12-Core Processor (3.79GHz)
- RAM: 20 GB
- Software: MATLAB 2020.

4.1 Benchmark functions' details

To adhere to these principles of validity and fairness, the benchmark testing suite employed in this study is publicly accessible. The benchmark function set is selected from 23 benchmark functions and IEEE CEC 2014. The full name of IEEE CEC 2014 is the IEEE Congress on Evolutionary Computation 2014 competition benchmark functions. These benchmark datasets facilitate assessing various algorithms' performance according to established standards. The function set contains several types of functions, including unimodal functions (F1-7, F14-15), multimodal functions (F8-13, F16-19), hybrid functions, and composition functions (F20-30). In the subsequent context, different types of functions are referred to as unimodal-f, multimodal-f, and hybrid/composition-f for brevity. The details of the benchmark function set are shown in Table 3.

Table 3 The detail of the benchmark function set

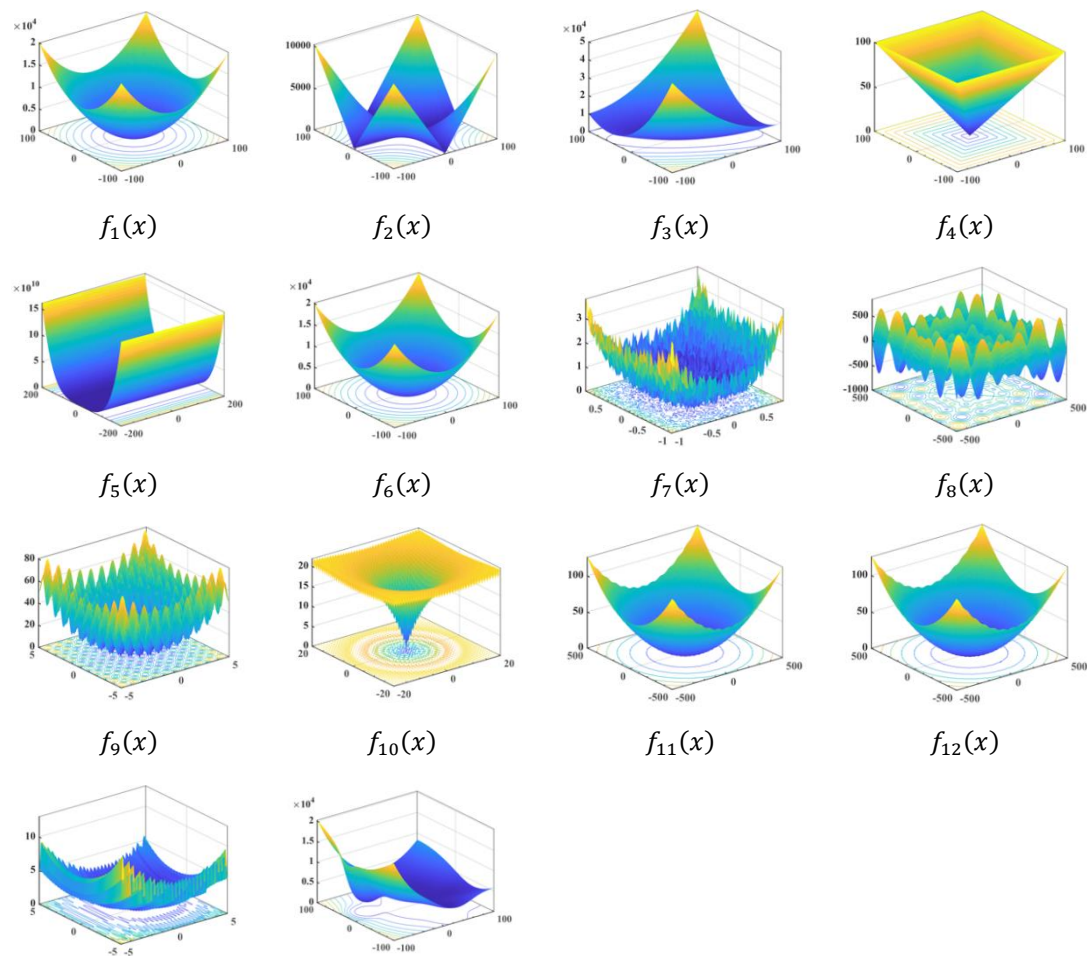
Function	Search range	f_{min}
$f_1(x) = \sum_{i=1}^n x_i^2$	[-100,100]	0
$f_2(x) = \sum_{i=1}^n x_i + \prod_{i=1}^n x_i $	[-10,10]	0
$f_3(x) = \sum_{i=1}^n (\sum_{j=1}^i x_j)^2$	[-100,100]	0

$f_4(x) = \max_i\{ x_i , 1 \leq i \leq n\}$	[-100,100]	0
$f_5(x) = \sum_{i=1}^{n-1}[100(x_{i+1} - x_i^2)^2 + (x_i - 1)^2]$	[-30,30]	0
$f_6(x) = \sum_{i=1}^n([x_i + 0.5])^2$	[-100,100]	0
$f_7(x) = \sum_{i=1}^n ix_i^4 + \text{random}[0,1]$	[-128,128]	0
$f_8(x) = \sum_{i=1}^n -x_i \sin(\sqrt{ x_i })$	[-500,500]	0
$f_9(x) = \sum_{i=1}^n [x_i^2 - 10 \cos(2\pi x_i) + 10]$	[-5.12, 5.12]	0
$f_{10}(x) = -20 \exp(-0.2 \sqrt{\frac{1}{n} \sum_{i=1}^n x_i^2}) - \exp(\frac{1}{n} \sum_{i=1}^n \cos(2\pi x_i)) + 20 + e$	[-32,32]	0
$f_{11}(x) = \frac{1}{4000} \sum_{i=1}^n x_i^2 - \prod_{i=1}^n \cos(\frac{x_i}{\sqrt{i}}) + 1$	[-600,600]	0
$f_{12}(x) = \frac{\pi}{n} \{10 \sin(\pi y_1) + \sum_{i=1}^n (y_i - 1)^2 [1 + 10 \sin^2(\pi y_{i+1})] + (y_n - 1)^2\} +$ $\sum_{i=1}^n u(x_i, 10, 100, 4)$, $y_i = 1 + \frac{x_i+1}{4}$	[-50,50]	0
$u(x_i, a, k, m) = \begin{cases} k(x_i - a)^m & x_i > a \\ 0 & -a < x_i < a \\ k(-x_i - a)^m & x_i < -a \end{cases}$		
$f_{13}(x) = 0.1\{\sin^2(3\pi x_1) + \sum_{i=1}^n (x_i - 1)^2 [1 + \sin^2(3\pi x_i + 1)] + (x_n - 1)^2 [1 + \sin^2(2\pi x_n)]\} + \sum_{i=1}^n u(x_i, 5, 100, 4)$	[-50,50]	0
$f_{14}(x)$ =Rotated High Conditional Elliptic Function	[-100,100]	100
$f_{15}(x)$ =Rotated Bent Cigar Function	[-100,100]	200
$f_{16}(x)$ =Shifted Rastrigin's Function	[-100,100]	800
$f_{17}(x)$ =Shifted and Rotated Katsuura Function	[-100,100]	1200
$f_{18}(x)$ =Shifted and Rotated HGBat Function	[-100,100]	1400
$f_{19}(x)$ =Shifted and Rotated Expanded Griewank's plus Rosenbrock's Function	[-100,100]	1500
$f_{20}(x)$ =Hybrid Function 1 (N=3)	[-100,100]	1700
$f_{21}(x)$ =Hybrid Function 2 (N=3)	[-100,100]	1800
$f_{22}(x)$ =Hybrid Function 4 (N=4)	[-100,100]	2000
$f_{23}(x)$ =Hybrid Function 5 (N=5)	[-100,100]	2100
$f_{24}(x)$ =Composition Function 1 (N=5)	[-100,100]	2300
$f_{25}(x)$ =Composition Function 2 (N=3)	[-100,100]	2400
$f_{26}(x)$ =Composition Function 3 (N=3)	[-100,100]	2500
$f_{27}(x)$ =Composition Function 5 (N=5)	[-100,100]	2700
$f_{28}(x)$ =Composition Function 6 (N=5)	[-100,100]	2800
$f_{29}(x)$ =Composition Function 7 (N=3)	[-100,100]	2900
$f_{30}(x)$ =Composition Function 8 (N=3)	[-100,100]	3000

Liang et al. [66] provided a detailed introduction to the continuous multimodal benchmark function dataset used in this study. To provide a more comprehensive description of this dataset,

Figure 12 and Table 4 respectively illustrate the distribution of the function search space and the mathematical properties of the functions.

Figure 12 clearly demonstrates the three-dimensional function search space of the multi-types in the function sets. In the figure, F_4 , as the representative of the unimodal-f, has an extreme value in the search space. Unimodal-f poses a great challenge to the local search capability and continuous optimization ability of optimization algorithms, as well as testing the search speed of the algorithms. While F_8 , as the representative of the multimodal-f, has multiple extreme values, Therefore, they also test the global search capability of the algorithms, demonstrating their ability to avoid getting trapped in local optima. Furthermore, the dataset includes hybrid and composition functions to test the algorithm's self-adaptation and adaptability when facing more complex function definition search spaces. The figure and the table showcase the unique properties of these types of functions. F_{24} combines the characteristics of unimodal and multimodal functions to represent the hybrid/composition-f. Furthermore, the functions F_{17} - F_{30} possess more complex properties, such as multi-modal, non-separable, asymmetrical, different properties around different local optima, and different properties for different variable subcomponents. These properties comprehensively test the optimization capability of the algorithms in a broader sense.



F12	8	10	9	7	4	6	3	5	1	2
F13	9	10	8	6	7	5	2	3	4	1
F14	9	10	4	5	6	2	7	1	3	8
F15	3	1	4	5	2	6	7	8	9	10
F16	2	1	3	4	5	6	8	7	10	9
F17	1	10	6	5	7	9	3	4	2	8
F18	1	4	6	2	7	10	5	9	8	3
F19	9	10	8	7	6	5	4	3	2	1
F20	4	10	9	6	3	2	1	5	8	7
F21	7	5	6	3	8	4	9	10	1	2
F22	9	10	8	4	2	1	7	5	6	3
F23	5	7	10	3	1	2	8	9	6	4
F24	1	1	1	1	1	1	1	1	1	1
F25	3	2	4	1	5	7	6	8	9	10
F26	1	1	1	1	1	1	1	1	1	1
F27	5	2	9	10	4	6	8	3	1	7
F28	5	9	1	6	7	8	10	2	4	3
F29	2	3	6	5	9	4	10	7	1	8
F30	10	9	3	8	5	1	6	7	2	4
Average	4.200	5.300	4.933	4.633	4.633	4.867	6.000	5.500	4.500	4.667
Rank	1	8	7	3	3	6	10	9	2	5

4.3 Qualitative analysis

The qualitative analysis experiments demonstrate the search rules and characteristics of FATA when dealing with different benchmark functions, including unimodal, multimodal, hybrid, and composition functions. Figure 13 gives the results of five different analyses: (a) The 3D plot of the benchmark function; (b) The population search history on the function corresponding to Figure 13a; (c) The trajectory of the agent on the function corresponding to Figure 13a; (d) The average fitness of all agents on the function corresponding to Figure 13a; and (e) The convergence curve of FATA on the function corresponding to Figure 13a. Among them, the 3D model of the benchmark functions in Figure 13a shows that F3 and F14 are unimodal functions. F13, F18, and F19 are multimodal functions. F24 is a composition function.

The search history in Figure 13b demonstrates the distribution of individuals in the search space. In Figure 13b, each black dot represents an individual in the population, and the unique red dot in each figure represents the optimal value in the search space. Based on the mirage principle, the FATA continuously balances the global exploration and local exploitation of population individuals. First, under the effect of the mirage light filtering principle, as shown in Figure 13b, the black dots representing individuals are widely distributed to perform searches in various corners of the search space. FATA executes the global search method at the benchmark function by following a slash

through the search space, as represented by the black diagonal line in Figure 13b. Then, under the light propagation strategy of the algorithm, the population black dots in the figure will gradually balance the global exploration and local exploitation methods and move towards the red optimal value. Meanwhile, the algorithm spreads the population into several local regions and searches them simultaneously to avoid the local optimum. As shown in F14 of the figure, the FATA jumps out of the local optimum and finds the optimal solutions in the boundary region.

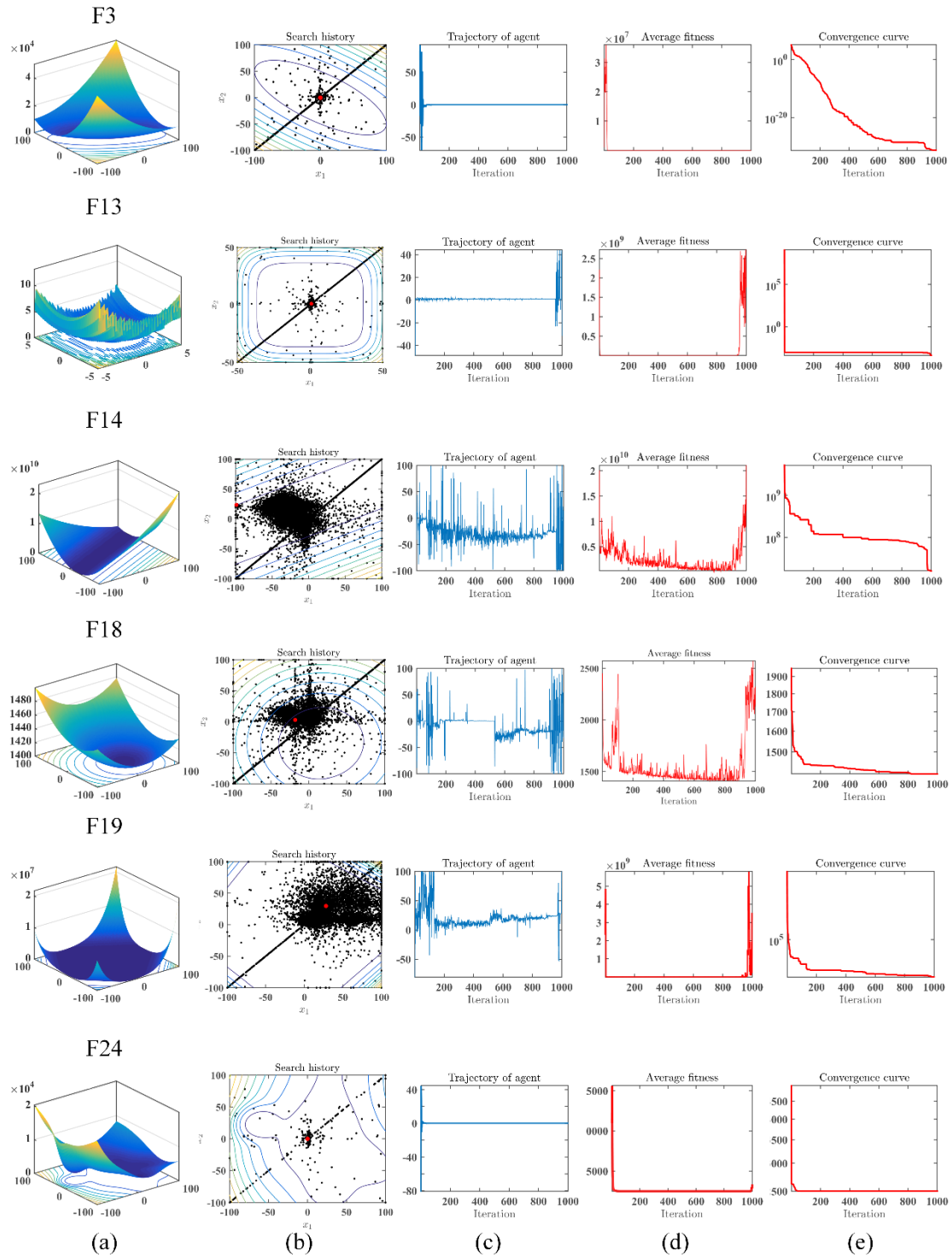


Figure 13. (a) The 3D plot of the benchmark function (b) Search history (c) Trajectory of agent (d) The

average fitness of all agents (e) The convergence curve of FATA

The trajectory of the light individual position change in Figure 13c represents the distance change curve in search of the optimal value and the process of continuously balancing global exploration and local exploitation in the algorithm. For example, in the case of F19, during the first 200 iterations, the FATA primarily conducts global exploration behavior, resulting in a significant change in the position of the light individual. However, from the 200th to the 800th iteration, the algorithm mainly utilizes a local exploitation strategy, leading to minimal changes in the position of the light individual. As the FATA continuously balances global exploration and local exploitation strategies, during the final 800 to 1000 iterations, the algorithm achieves an optimal balance between global exploration and local exploitation strategies, assisting in finding the optimal value for the F19 multimodal function.

On F3, F13, F18, F19, and F24, the individual search distance reaches 50% of the search space to improve the convergence speed of the algorithm. Meanwhile, the algorithm falls into a local optimum in the early F14 period, but the global exploration and local exploitation of the equilibrium in the later phase help the algorithm find the optimal value. Different search characteristics of various functions reflect the adaptability and robustness of the FATA to different types.

Figure 13d shows the trend of population quality during the optimization process. Although the average fitness curve of the algorithm oscillates in the early stages, the oscillation is a decreasing trend. This shows that the algorithm continuously improves the quality of the algorithm population in the process of balancing global exploration and local exploitation. Meanwhile, the population fitness oscillations of the algorithm at the lately evolving stage become larger in magnitude on functions such as F13, F14, etc., demonstrating the algorithm's behavior of trying to move beyond the LO at the lately evolving stage. The minimum fitness value decreases gradually with the number of iterations in Figure 13e. In F3, F13, and F14, the FATA can jump out of the local optimum.

4.4 Algorithm's exploitation analysis on unimodal-f

The unimodal function has only one extreme value in the search space, which tests the algorithm's exploitation search. This section shows the experimental results of FATA with other comparative algorithms for solving nine unimodal functions (F1–7, F14–15) in the function set.

Table 6 and Table A.1 show the average (AVG) and the standard deviation (STD), which verify the algorithm's optimization results and stability. The best-performing algorithms for each function's data are identified in bold font in the tables. Table 6 shows the results of FATA and classic comparative algorithms. FATA obtains good rankings for STD and AVG on F1-3 and F5 in Table 6. Table A.1 shows the results of FATA and improved comparative algorithms. FATA is ranked first or second on AVG and STD when solving F1-3, F5, F6, F14, and F15 in Table A.1. So, experimental results demonstrate that FATA obtains more stable and accurate optimization results than its excellent

counterparts in the algorithm's exploitation analysis experiment. Furthermore, to ensure the reliability of the experimental results, this section also employed the p-value analysis method of WSRT to perform statistical tests on the experimental results. Table A.2 and Table A.3 present the p-values obtained from the WSRT for two sets of experiments comparing FATA with classical algorithms and improved algorithms, respectively. P-values greater than 0.05 are marked in bold in the tables; this indicates that the experimental results are reliable. It can be observed that comparative algorithms obtain p-values less than 0.05 on most of the unimodal functions, which means that the proposed algorithm is statistically significant for the experimental results. Therefore, the experimental results in this section verify that FATA has competitive and stable exploitation capabilities.

Table 6 Results of FATA and classic algorithms on the unimodal functions

	F1		F2		F3	
	AVG	STD	AVG	STD	AVG	STD
FATA	0.0000E+00	0.0000E+00	5.7971E-194	0.0000E+00	0.0000E+00	0.0000E+00
MVO	3.1447E-03	8.2520E-04	4.2472E-02	1.4725E-02	4.0052E-01	1.5567E-01
SCA	1.2820E-52	7.0215E-52	5.9622E-59	2.9276E-58	2.1836E-01	4.9810E-01
AOA	0.0000E+00	0.0000E+00	0.0000E+00	0.0000E+00	0.0000E+00	0.0000E+00
GSA	1.5044E+01	1.7095E+00	1.5595E+01	9.5325E-01	3.1098E+02	6.1801E+01
DE	2.3814E-159	6.8707E-159	2.1719E-94	2.6752E-94	1.5196E+03	7.2547E+02
ACOR	3.2039E-179	0.0000E+00	3.3333E-01	1.8257E+00	1.0000E+03	2.0342E+03
PSO	9.8938E+01	1.1542E+01	4.5962E+01	3.5116E+00	1.8061E+02	2.9787E+01
WOA	0.0000E+00	0.0000E+00	0.0000E+00	0.0000E+00	3.1560E+01	6.3813E+01
CSA	1.3013E-14	8.0209E-15	1.3632E+00	8.9869E-01	7.7885E-05	7.0868E-05
	F4		F5		F6	
	AVG	STD	AVG	STD	AVG	STD
FATA	8.5691E-04	1.2803E-03	2.2795E-02	3.5061E-02	1.3585E-04	8.9892E-05
MVO	9.7945E-02	3.9819E-02	1.4538E+02	2.4070E+02	3.0164E-03	8.1301E-04
SCA	1.8623E-02	8.4115E-02	2.7488E+01	7.1405E-01	3.5911E+00	2.5795E-01
AOA	0.0000E+00	0.0000E+00	2.3040E+01	4.6221E-01	4.0501E-01	8.4926E-02
GSA	1.7233E+00	1.3553E-01	9.4189E+03	2.1305E+03	1.5808E+01	1.4970E+00
DE	2.1964E-14	6.0884E-14	4.0296E+01	2.5111E+01	0.0000E+00	0.0000E+00
ACOR	3.8620E+01	7.9879E+00	2.7381E+01	5.1565E+01	3.4217E-29	1.2699E-28
PSO	3.7208E+00	2.3008E-01	8.8866E+04	1.9336E+04	9.7401E+01	1.3001E+01
WOA	3.0502E+00	8.7069E+00	2.4349E+01	2.5253E-01	6.4429E-06	3.1204E-06
CSA	5.1300E-01	5.0880E-01	3.4568E+01	2.1199E+01	1.4021E-14	1.0363E-14
	F7		F14		F15	
	AVG	STD	AVG	STD	AVG	STD
FATA	3.37618E-05	2.71768E-05	1.1882E+07	6.3001E+06	9.9120E+07	4.8585E+07
MVO	0.003038325	0.00090622	3.2340E+06	1.0856E+06	2.0380E+04	1.1871E+04
SCA	0.002196096	0.002338581	2.3217E+08	6.5937E+07	1.6308E+10	2.6998E+09
AOA	1.07912E-07	9.69345E-08	6.7841E+07	4.0822E+07	1.9886E+10	4.6029E+09
GSA	30.31046008	4.269074104	1.3517E+06	4.3468E+05	2.0937E+07	2.4741E+06
DE	0.002625521	0.000485205	1.8993E+07	4.5362E+06	1.3254E+03	4.0100E+03

ACOR	0.094640039	0.489903343	4.0891E+06	7.0704E+06	4.8199E+07	2.6392E+08
PSO	109.2657232	28.13238689	8.3533E+06	2.8085E+06	1.4803E+08	1.3750E+07
WOA	0.000182642	0.000210106	3.0331E+07	1.2600E+07	7.4729E+06	1.2604E+07
CSA	0.005909227	0.002188262	2.2623E+06	1.5976E+06	1.0192E+04	6.2266E+03

4.5 Algorithm's exploration analysis on multimodal-f

The multimodal function has multiple extremes in the search space, testing the algorithm's global exploration ability. So, this section shows the experimental results of the FATA and other comparison algorithms based on ten multimodal functions (F8–13, F16–19) in the function set to analyze the exploration performance.

Table 7 shows the STD and AVG analysis results of FATA and other original algorithms. FATA obtains excellent AVG or STD rankings on multimodal functions such as F8, F9, and F11. The classical SCA, PSO, and the new algorithm CSA do not perform well in the experiment. Moreover, the FATA obtained better experimental results than DE. Table A.4 illustrates that FATA can maintain certain advantages over its improved counterparts on F8-9, F11-13, F16, and F18-19. The analysis results demonstrate the proposed algorithm's better stability and optimal solutions for tackling multimodal functions. In Tables A.5 and A.6, the p-values of the comparison algorithms are less than 0.05 for most of the multimodal functions. Therefore, FATA is highly reliable for comparison. The relevant experimental results prove that FATA is competitive in exploration. However, the performance of the FATA on F17 is slightly lower than others, according to the “no free lunch” theorem. So, there is still room for improvement in controlling global search.

Table 7 Results of FATA and classic algorithms on the multimodal functions

Function	F8		F9	
	AVG	STD	AVG	STD
FATA	-1.2569E+04	3.7771E-04	0.0000E+00	0.0000E+00
MVO	-8.1960E+03	6.5217E+02	9.0609E+01	2.3168E+01
SCA	-4.4665E+03	3.2075E+02	2.1582E+00	8.2132E+00
AOA	-1.0729E+04	4.5967E+02	0.0000E+00	0.0000E+00
GSA	-2.6533E+03	5.3378E+02	1.9988E+02	1.1820E+01
DE	-1.2420E+04	1.3631E+02	3.3165E-02	1.8165E-01
ACOR	-8.4294E+03	4.8538E+02	4.0174E+01	2.7452E+01
PSO	-6.9852E+03	9.0693E+02	3.4778E+02	1.9697E+01
WOA	-1.2221E+04	9.9278E+02	0.0000E+00	0.0000E+00
CSA	-6.8296E+03	9.5861E+02	2.5803E+01	1.1482E+01
Function	F10		F11	
	AVG	STD	AVG	STD
FATA	3.0114E-04	5.0770E-04	0.0000E+00	0.0000E+00
MVO	1.0776E-01	3.5784E-01	2.4967E-02	1.0328E-02
SCA	9.0753E+00	9.3734E+00	1.7340E-09	9.4973E-09

AOA	8.8818E-16	0.0000E+00	3.3484E-03	1.2891E-02
GSA	4.1651E+00	1.7825E-01	5.4657E-01	5.2436E-02
DE	7.5199E-15	1.2283E-15	0.0000E+00	0.0000E+00
ACOR	2.2963E-01	5.3440E-01	9.1887E-03	9.9603E-03
PSO	7.7567E+00	3.4324E-01	1.0158E+00	1.0416E-02
WOA	3.6119E-15	2.5861E-15	7.3602E-04	2.8740E-03
CSA	3.8179E+00	8.2261E-01	1.2791E-02	1.6262E-02
Function	F12		F13	
	AVG	STD	AVG	STD
FATA	1.0013E-06	7.3144E-07	1.7016E-05	1.6450E-05
MVO	9.0524E-02	2.8587E-01	4.0379E-03	5.3826E-03
SCA	3.7486E-01	1.3290E-01	2.0523E+00	9.6713E-02
AOA	9.9453E-03	3.3374E-03	2.2315E+00	2.8461E-01
GSA	1.4696E+00	3.3443E-01	8.2058E+00	1.0078E+00
DE	1.5705E-32	5.5674E-48	1.3498E-32	5.5674E-48
ACOR	1.0025E-01	2.1876E-01	4.7294E-01	1.2000E+00
PSO	3.3744E+00	4.4042E-01	1.5402E+01	1.4452E+00
WOA	1.0851E-06	5.7971E-07	1.1246E-03	3.3487E-03
CSA	1.9513E+00	1.8813E+00	1.9807E-02	2.7325E-02
Function	F16		F17	
	AVG	STD	AVG	STD
FATA	8.9109E+02	1.2859E+01	1.2018E+03	4.9301E-01
MVO	8.7697E+02	2.6619E+01	1.2002E+03	8.8716E-02
SCA	1.0396E+03	1.6041E+01	1.2025E+03	2.6517E-01
AOA	9.4869E+02	1.3345E+01	1.2005E+03	1.6466E-01
GSA	8.3857E+02	5.7730E+00	1.2009E+03	1.3472E-01
DE	8.0110E+02	1.3298E+00	1.2009E+03	1.3229E-01
ACOR	8.5947E+02	1.6591E+01	1.2025E+03	2.5133E-01
PSO	9.7082E+02	2.0279E+01	1.2025E+03	2.7180E-01
WOA	9.8578E+02	4.7846E+01	1.2017E+03	4.8017E-01
CSA	9.4155E+02	2.2777E+01	1.2008E+03	3.2855E-01
Function	F18		F19	
	AVG	STD	AVG	STD
FATA	1.4006E+03	3.2400E-01	1.5764E+03	3.9344E+01
MVO	1.4005E+03	3.1318E-01	1.5075E+03	3.1935E+00
SCA	1.4442E+03	8.1307E+00	4.1046E+03	2.2708E+03
AOA	1.4612E+03	1.6279E+01	2.0317E+03	1.9916E+02
GSA	1.4003E+03	4.0510E-02	1.5129E+03	9.5062E-01
DE	1.4003E+03	4.7398E-02	1.5114E+03	1.1321E+00
ACOR	1.4007E+03	3.1200E-01	1.5337E+03	7.1596E+01
PSO	1.4003E+03	1.5126E-01	1.5166E+03	1.1045E+00
WOA	1.4003E+03	4.8360E-02	1.5722E+03	2.9409E+01
CSA	1.4003E+03	4.7321E-02	1.5273E+03	1.0043E+01

4.6 Algorithm circumvented LO analysis in hybrid/composition-f

This section shows the experimental results of FATA and other comparative algorithms on 11 hybrid and composition functions in the function set. These functions have a complex search space that tests the ability to escape from the local optimum.

According to the data in Table 8, FATA is ranked first on AVG or STD when solving F24-F29, which shows the algorithm's potential to jump out of the local optimum. Table A.7 also shows the results of STD and AVG analyses obtained by FATA and other improved algorithms. The FATA also obtains better rankings than others. The comparative algorithms include classical algorithms, novel algorithms, and improved algorithms. Therefore, the experimental results show that FATA can steadily optimize these functions and provide better solutions. The ability of the algorithm to jump out of the local optimum is also verified. At the same time, the convergence speed of the algorithm is accelerated. Meanwhile, in Tables A.8 and A.9, other comparison algorithms obtain p-values less than 0.05 on most of the hybrid and composition functions, which indicates that the results have significant reliability.

Table 8 Results of FATA and classic algorithms on the hybrid/composite functions

Item	F20		F21		F22	
	AVG	STD	AVG	STD	AVG	STD
FATA	6.2621E+05	4.1299E+05	2.3030E+04	6.7980E+04	5.3567E+03	3.9462E+03
MVO	1.7501E+05	9.2088E+04	1.3302E+04	1.0176E+04	2.3051E+03	8.7293E+01
SCA	5.9308E+06	2.5974E+06	1.6911E+08	9.0962E+07	1.5174E+04	4.2875E+03
AOA	5.7836E+04	3.1540E+04	4.8117E+03	2.0849E+03	3.0008E+04	1.0710E+04
GSA	2.1708E+05	1.3318E+05	7.1558E+04	2.0933E+04	3.6254E+04	1.6074E+04
DE	1.6015E+06	6.5371E+05	8.5495E+03	5.5899E+03	5.4357E+03	1.9712E+03
ACOR	9.6408E+04	1.2143E+05	6.0428E+03	6.3779E+03	3.9351E+03	3.6175E+03
PSO	2.7027E+05	1.4735E+05	2.0667E+06	6.3285E+05	2.3032E+03	6.8868E+01
WOA	4.7161E+06	2.5544E+06	5.5528E+03	3.7023E+03	2.8383E+04	1.7439E+04
CSA	1.1933E+04	8.4243E+03	2.2697E+03	6.4178E+02	2.4141E+03	1.7014E+02
Item	F23		F24		F25	
	AVG	STD	AVG	STD	AVG	STD
FATA	3.6894E+05	3.1391E+05	2.5000E+03	8.4444E-14	2.6000E+03	3.0789E-04
MVO	6.0303E+04	4.2731E+04	2.6155E+03	1.8819E-01	2.6267E+03	6.3285E+00
SCA	1.4026E+06	7.3481E+05	2.6685E+03	1.2184E+01	2.6001E+03	6.2765E-02
AOA	2.7720E+04	9.6563E+03	2.5767E+03	6.3680E+01	2.6000E+03	0.0000E+00
GSA	1.2284E+05	6.3010E+04	2.6156E+03	3.5321E+00	2.6082E+03	5.0283E-01
DE	2.5842E+05	9.6325E+04	2.6152E+03	1.3876E-12	2.6261E+03	3.4373E+00
ACOR	3.8593E+04	4.1166E+04	2.6176E+03	4.8962E+00	2.6396E+03	8.5355E+00
PSO	1.2364E+05	9.1541E+04	2.6158E+03	3.7768E-01	2.6290E+03	4.0172E+00
WOA	1.4174E+06	1.0908E+06	2.6341E+03	1.0633E+01	2.6040E+03	3.4011E+00
CSA	1.4046E+04	5.7940E+03	2.6168E+03	9.5294E-01	2.6192E+03	1.0535E+01
Item	F26		F27		F28	
	AVG	STD	AVG	STD	AVG	STD

Item	AVG	STD	AVG	STD	AVG	STD
FATA	2.7000E+03	8.4444E-14	2.9000E+03	6.2496E-03	3.0000E+03	1.0133E-02
MVO	2.7054E+03	1.6810E+00	3.2534E+03	1.1575E+02	3.8616E+03	2.0509E+02
SCA	2.7262E+03	6.7005E+00	3.4872E+03	3.5061E+02	4.8966E+03	4.1790E+02
AOA	2.7000E+03	0.0000E+00	3.1151E+03	4.1905E+02	4.0838E+03	1.4729E+03
GSA	2.7019E+03	1.1607E-01	3.2073E+03	1.1199E+02	4.7128E+03	3.3843E+02
DE	2.7072E+03	8.0592E-01	3.2160E+03	6.7931E+01	3.6337E+03	2.4785E+01
ACOR	2.7071E+03	4.3186E+00	3.3651E+03	1.0291E+02	3.8822E+03	1.7618E+02
PSO	2.7124E+03	5.4852E+00	3.4906E+03	2.7829E+02	6.9969E+03	6.6428E+02
WOA	2.7167E+03	1.4805E+01	3.6689E+03	4.0827E+02	4.9677E+03	5.4518E+02
CSA	2.7091E+03	3.8509E+00	3.1067E+03	7.3723E+00	6.4428E+03	6.9324E+02
	F29		F30			
Item	AVG	STD	AVG	STD		
FATA	8.3696E+03	1.6576E+04	6.5367E+03	5.4372E+03		
MVO	4.1917E+05	2.1920E+06	8.3250E+03	2.1778E+03		
SCA	1.1400E+07	7.8961E+06	2.5335E+05	8.0388E+04		
AOA	5.7588E+07	7.5894E+07	7.4386E+04	1.3536E+05		
GSA	2.8770E+07	5.3075E+07	7.9336E+03	9.2391E+02		
DE	2.5319E+05	1.3601E+06	6.2523E+03	9.9588E+02		
ACOR	1.4381E+06	3.6882E+06	1.1370E+04	9.4062E+03		
PSO	2.6253E+04	4.8327E+04	1.4577E+04	5.9262E+03		
WOA	6.2335E+06	4.5092E+06	8.3335E+04	6.8178E+04		
CSA	3.8079E+06	1.4477E+07	1.7481E+04	2.6219E+04		

4.7 Comparison with the best-performing champion algorithms

To test the performance of FATA more objectively, it is compared with the improved DEs, the improved PSOs, and the 2017 winners on the multi-type function set. The improved DEs, PSOs, and 2017 winners are the best-performing algorithms in the swarm intelligence algorithms. Table A.10 shows the results of the data analysis for this experiment. Among them, FATA obtains the optimal STD and AVG values for functions such as F1, F4, and F20. As a result, FATA can obtain more stable and accurate performance on many types of functions than its counterparts.

Table 9 shows the WSRT p-values acquired by the experimental results. In the table, FATA outperforms (+) the MPEDE and LSHDE in 14 functions. FATA performs similarly to MPEDE and LSHDE in 11 and 12 functions, respectively. Because the p-values obtained by the comparison algorithm in the experiment are less than 0.05, all the proposed algorithm obtains experimental results with significant reliability. So, FATA shows competitiveness in comparison with excellent algorithms.

From Figure 14, FATA outperforms several DE-improved algorithms, PSO-improved algorithms, and 2017 winners on functions such as F3, F5, F24, and F28. The combined experimental results show that the design of FATA is valuable and necessary.

Table 9 The statistical results of FATA versus other peers

	EPSO	ASCA_PSO	SCADE	SADE	MPEDE	LSHADE
F1	0.0000017344	0.0000017344	1.0000000000	0.0000017333	0.0000017333	0.0000017344
F2	0.0000017344	0.0000017344	0.0000017344	0.0000017344	0.0000017344	0.0000017344
F3	0.0000017344	0.0000017344	1.0000000000	0.0000017344	0.0000017344	0.0000017344
F4	0.0000069838	0.0000017344	0.0000017344	0.0043896183	0.0000102463	0.0005287248
F5	0.0000017344	0.0000017344	0.0005287248	0.0000017344	0.3820341630	0.1650265656
F6	0.0000017344	0.0000017344	0.0000017344	0.0000017344	0.0000017344	0.0000017344
F7	0.0000017344	0.0000017344	0.0000038822	0.0000017344	0.0000017344	0.0000017344
F8	0.0000017344	0.0000017344	0.0000017344	0.0147954242	0.0000017344	0.0300098913
F9	0.0000017344	0.0000017344	1.0000000000	0.0002896194	0.0000017322	0.0004882813
F10	0.0146332985	0.0000017344	0.0000049202	0.0000234563	0.0000069760	0.0000017344
F11	0.0001863266	0.0000017344	1.0000000000	0.0002441406	0.0001957504	0.0000017333
F12	0.0000017344	0.0000017344	0.0000017344	0.0147954242	0.0036094333	0.0006156406
F13	0.0000017344	0.0000017344	0.0000017344	0.0003588845	0.3820341630	0.0000076909
F14	0.0001056950	0.0002411796	0.0000017344	0.0000017344	0.0000017344	0.0000017344
F15	0.0000017344	0.0002830789	0.0000017344	0.0000017344	0.0000017344	0.0000017344
F16	0.0110792291	0.0000017344	0.0000017344	0.0000017344	0.0000017344	0.0000017344
F17	0.0117481063	0.0000486026	0.0000021266	0.0000017344	0.0000017344	0.0000017344
F18	0.6435165948	0.0195692152	0.0000017344	0.0036094333	0.3820341630	0.1713763888
F19	0.0000019209	0.0000023534	0.0000017344	0.0000017344	0.0000017344	0.0000019209
F20	0.0002613431	0.0008307070	0.0000017344	0.0000017344	0.0000017344	0.0000017344
F21	0.0000035152	0.0000017344	0.0000017344	0.0000017344	0.0000017344	0.0000017344
F22	0.0001604638	0.0544625040	0.0000017344	0.0068358564	0.0000021266	0.0000063391
F23	0.0000818775	0.2536440975	0.0000017344	0.0000017344	0.0000017344	0.0000017344
F24	0.0000000432	0.0000017344	1.0000000000	0.0000000432	0.0000000432	0.0000017344
F25	0.0000017344	0.0000017344	0.0000017344	0.0000017344	0.0000017344	0.0000017344
F26	0.0000017344	0.0000017344	1.0000000000	0.0000017344	0.0000017344	0.0000017344
F27	0.0000017344	0.0000017344	0.0000136011	0.0000017344	0.0000017344	0.0000017344
F28	0.0000017344	0.0000017344	0.0000047292	0.0000017344	0.0000017344	0.0000017344
F29	0.4779474386	0.0000017344	0.0000017344	0.4048347222	0.0598356014	0.1588554993
F30	0.3285710736	0.0000057517	0.0000017344	0.3820341630	0.5440062076	0.5577426862
+/-/	14/13/3	27/1/2	17/7/6	17/11/2	14/11/5	14/12/4
=						

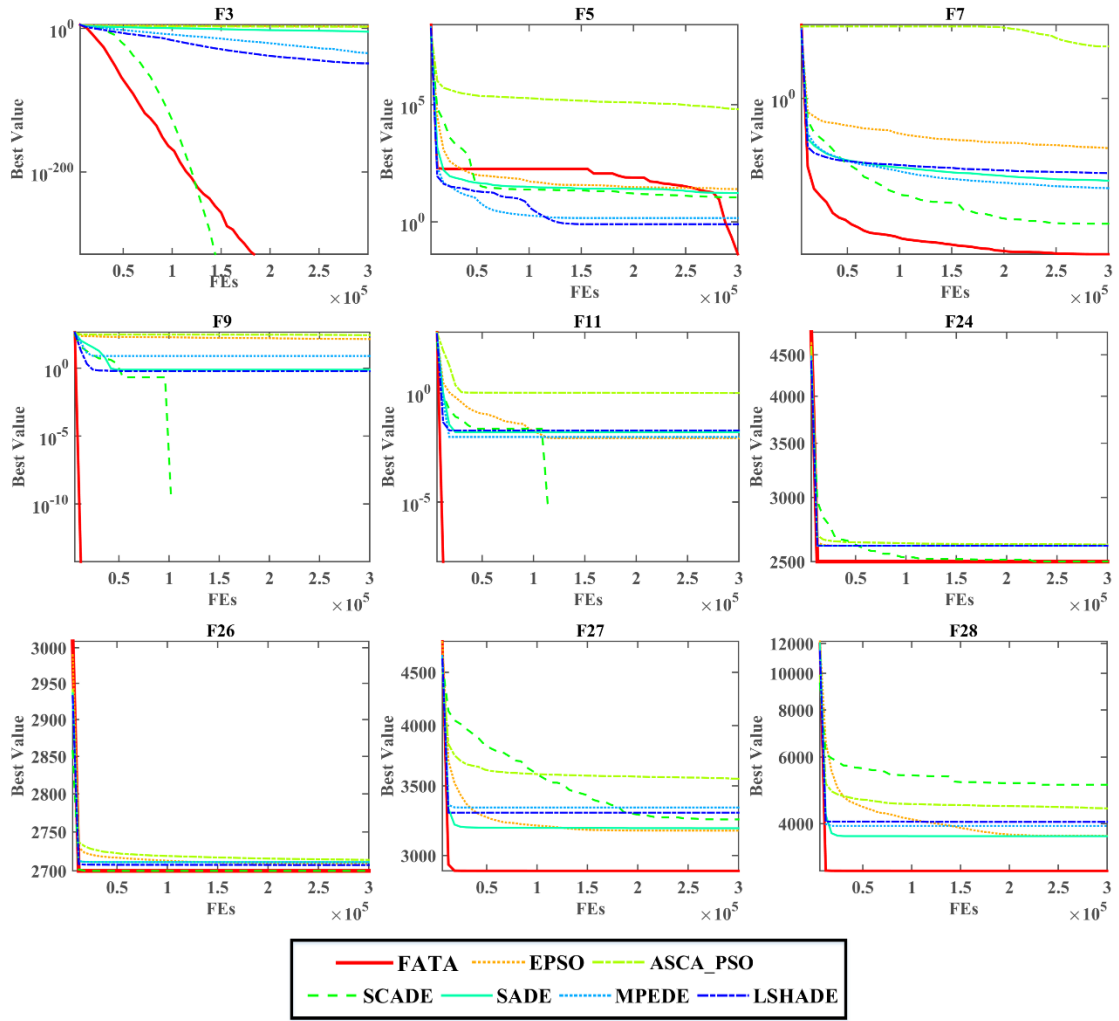


Figure 14. Comparisons between FATA and counterparts

4.8 Comparison with classical algorithms

To demonstrate the algorithm's overall performance when facing classical algorithms in the history of swarm intelligence algorithms, this section completes a comparative experiment of FATA and its counterparts on the entire function set. The WSRT, the FT, the convergence curve, and the computational cost analyze the experimental results of the functions.

First, Table 10 shows the results of the WSRT analysis in this comparison experiment, comparing the FATA and classical original counterparts. “+” means that the algorithm performs better than others. In the table, FT’s analysis result (mean) is “No.1.”. WSRT’s analysis result is also “No.1.”. The proposed FATA Friedman test is 4.175. The results show that FATA is better than its counterpart. Both results demonstrate a significant advantage of the proposed algorithm over others. Meanwhile, FATA outperformed (+) the DE in 14 functions on the function set. The FATA outperformed (+) the PSO in 24 functions. FATA outperformed the (+) physics-based algorithm, MVO, in 19 functions.

Table 10 The results of WSRT in this experiment

	FATA	MVO	SCA	AOA	GSA	DE	ACOR	PSO	WOA	CSA
+/-/	~	19/8/	28/0/2	14/9/7	21/8/1	14/10/	18/8/4	24/6/0	18/6/	20/10/
=		3				6			6	0
Mean	4.175	5.871	8.406	5.072	7.483	4.707	5.698	8.481	6.237	5.93
Rank	1	5	9	3	8	2	4	10	7	6

To show the performance of FATA more visually, Figure 15 presents the convergence curves of FATA and classical original peers on the functions F3, F5, F8, F24, F25, F26, F27, F28, and F29. The curves in the figure show the optimization process of FATA so that the algorithm can converge quickly to the optimal solution and avoid getting trapped in a local optimum. The analysis of experimental results in this section demonstrates the comprehensiveness of FATA on the multi-type function set.

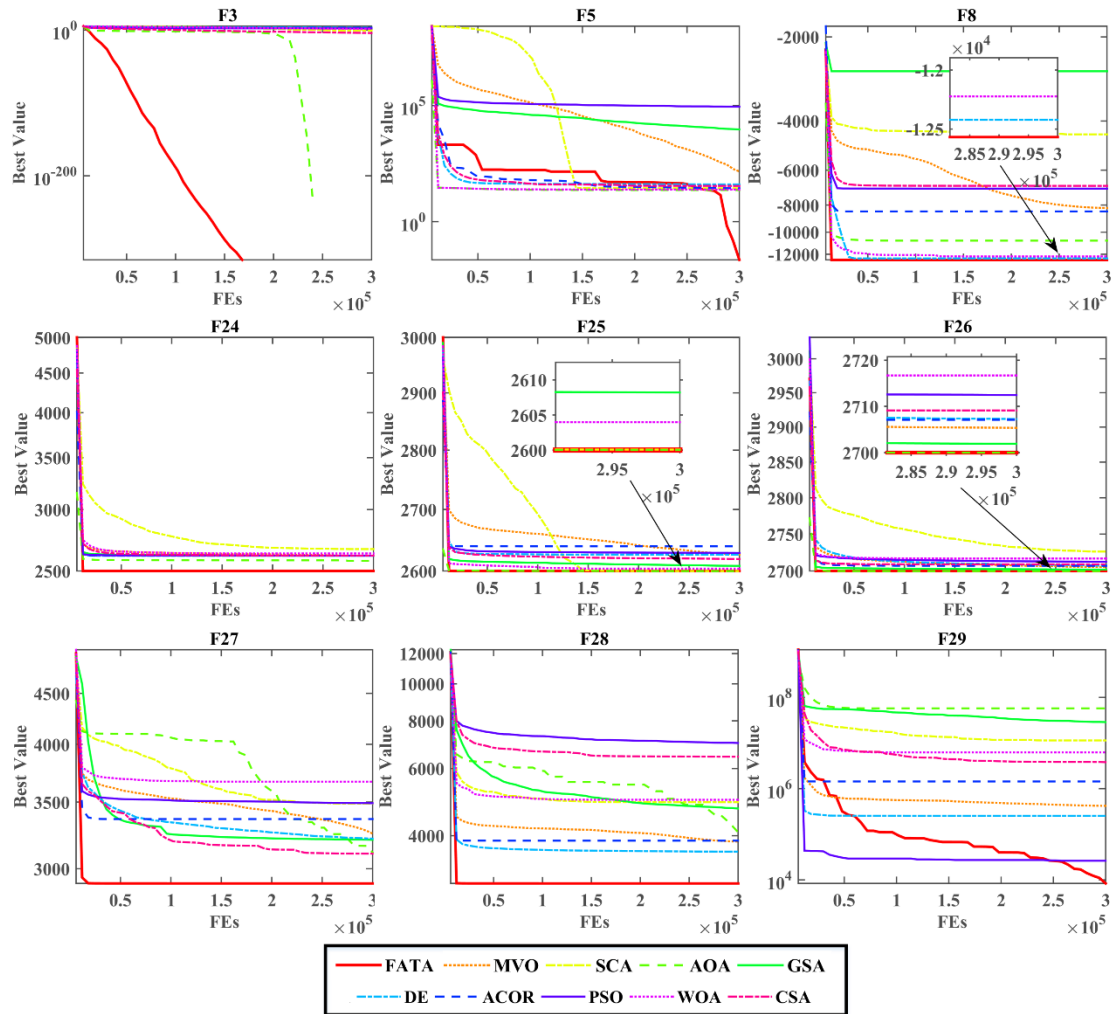


Figure 15. Comparisons between FATA and original counterparts

4.9 Comparison with state-of-the-art algorithms

To verify the competitiveness of the FATA among state-of-the-art algorithms (SOTA), this section compares the FATA with the recently proposed meta-heuristic algorithms: the rime optimization algorithm (RIME) [63], the liver cancer algorithm (LCA) [28], and the HHO [64]. Furthermore, the FATA is compared with the latest SOTA improved algorithms: XMACO [65], ACWOA, m_SCA, HGWO, CGSCA, AMFOA, DSMFO, and SFOA. The FATA is subjected to two experiments of the same type to demonstrate its performance.

Table 11 The WSRT^r results of FATA with SOTA algorithms

	FATA	RIME	HHO	LCA	XMACO
+/-/=	~	20/9/1	8/8/14	29/0/1	19/8/3
Mean	2.136	3.237	2.178	4.377	3.073
Rank	1	4	2	5	3

First, Table A.11 analyzes the experimental results of data statistics (STD and AVG) for the FATA and other algorithms such as RIME, HHO, LCA, and XMACO. To highlight the strengths and weaknesses of FATA compared to other optimizers in solving multi-type continuous functions. In the experiments, FATA achieved the best STD and AVG values in four out of nine unimodal functions in the function set, while obtaining suboptimal values in three other unimodal functions. In the set of eleven hybrid/composition functions, FATA achieved the best values in seven functions. The experimental results demonstrate that FATA exhibits stronger local exploitation and global exploration capabilities in solving unimodal and hybrid/composition functions when dealing with multi-type continuous function sets. However, the FATA shows weaker performance in optimizing multimodal functions, particularly in solving problems with search domains containing multiple optima.

Table 12 The results of WSRT^r results of FATA with improved algorithm

	FATA	ACWOA	m_SCA	HGWO	CGSCA	AMFOA	DSMFO	SFOA
+/-/=	~	17/6/7	22/3/5	20/6/4	16/7/7	23/5/2	15/9/6	24/4/2
Mean	3.818	4.603	5.636	5.535	4.978	7.984	4.829	8.461
Rank	1	2	6	5	4	7	3	8

Table 13 P-value of the experiment

	RIME	HHO	LCA	XMACO
F1	1.73440E-06	1.00000E+00	1.73440E-06	1.73440E-06
F2	1.73440E-06	1.00000E+00	1.73440E-06	1.73440E-06
F3	1.73440E-06	1.00000E+00	1.73440E-06	1.73440E-06
F4	1.73440E-06	1.00000E+00	1.73440E-06	1.73440E-06
F5	1.73440E-06	3.18168E-06	1.02463E-05	1.73440E-06
F6	1.73440E-06	1.92092E-06	1.73440E-06	1.73440E-06
F7	1.73440E-06	6.89229E-05	4.04835E-01	1.73440E-06
F8	1.73440E-06	2.84342E-05	1.73440E-06	1.73440E-06

F9	1.73440E-06	1.00000E+00	1.73440E-06	1.73440E-06
F10	1.73440E-06	1.00000E+00	1.73440E-06	1.39499E-06
F11	1.73440E-06	1.00000E+00	1.73440E-06	5.94168E-05
F12	1.73440E-06	5.75165E-06	1.73440E-06	6.43517E-01
F13	2.35342E-06	4.28569E-06	2.12664E-06	1.02011E-01
F14	1.73440E-06	4.52807E-01	1.73440E-06	1.73440E-06
F15	1.73440E-06	1.73440E-06	1.73440E-06	1.73440E-06
F16	1.73440E-06	5.98356E-02	1.73440E-06	1.96458E-03
F17	1.73440E-06	5.71646E-01	1.73440E-06	2.60333E-06
F18	5.85712E-01	2.30381E-02	1.73440E-06	1.98610E-01
F19	1.73440E-06	1.23808E-05	1.73440E-06	1.73440E-06
F20	9.84214E-03	2.22483E-04	1.73440E-06	7.69086E-06
F21	4.38962E-03	2.59671E-05	1.73440E-06	4.86026E-05
F22	1.73440E-06	3.72426E-05	1.73440E-06	4.49189E-02
F23	7.15703E-04	2.56371E-02	1.73440E-06	6.15641E-04
F24	1.73440E-06	1.00000E+00	1.73440E-06	1.01347E-07
F25	1.73440E-06	4.90825E-04	1.73440E-06	1.73440E-06
F26	1.73440E-06	1.00000E+00	1.73440E-06	1.73440E-06
F27	1.73440E-06	6.10352E-05	1.73440E-06	1.73440E-06
F28	1.73440E-06	1.00000E+00	1.73440E-06	1.73440E-06
F29	1.73440E-06	2.50000E-01	1.73440E-06	1.73440E-06
F30	1.73440E-06	1.56250E-02	1.73440E-06	1.73440E-06

Table 11 and Table 12 show the results of the WSRT analysis in this comparison experiment. Comparing the FATA and RIME, LCA, HHO, ACWOA, m_SCA, and SFOA, the WSRT ranking of FATA is No.1. Also, the FT score of FATA is 2.136/3.818. However, the FT score of the RIME is 3.237. That demonstrates the significant advantages of the algorithm over its other SOTA counterparts. Meanwhile, FATA outperformed (+) the RIME on 20 functions. FATA performs much better on the set of functions than the LCA, m_SCA, AMFOA, and SFOA algorithms. Furthermore, through the WSRT and data statistical analysis of the FATA and other comparative algorithms in solving multi-type continuous functions in the experiment, the FATA demonstrates comprehensive capabilities in solving various types of functions compared to classical algorithms, state-of-the-art algorithms, or excellent improved algorithms. As a result, FATA achieves the best WSRT results for the majority of multi-type continuous functions in the dataset.

Table 13 displays the P-value values obtained by the comparative algorithms RIME, LCA, HHO, and XMACO in this experiment. The data in the table indicates that the P-value values obtained by these four algorithms on most functions are less than or equal to 0.05, confirming the reliability of the statistical results in this experiment. To show the performance of FATA more visually, Figure 16 presents the convergence curves of FATA, RIME, LCA, and HHO on the functions F3, F7, F25, F26, F29, and F30. Figure 17 presents the convergence curves of FATA and its original peers on the

functions F3, F5, F8, F24, F25, F26, F27, F28, and F29. The curves in the figure show the optimization process of FATA so that the algorithm can converge quickly to the optimal solution and avoid getting trapped in a local optimum. Then, in Figure 17, when facing the excellent state-of-the-art algorithm, FATA demonstrates better convergence and accuracy in solving unimodal functions and hybrid/composition functions (F3, F5, F8, F24, F25, and F26). FATA shows competitiveness in solving multi-type functions. Owing to its formidable optimization prowess, the proposed FATA exhibits adaptability appropriate for an extensive array of applications.

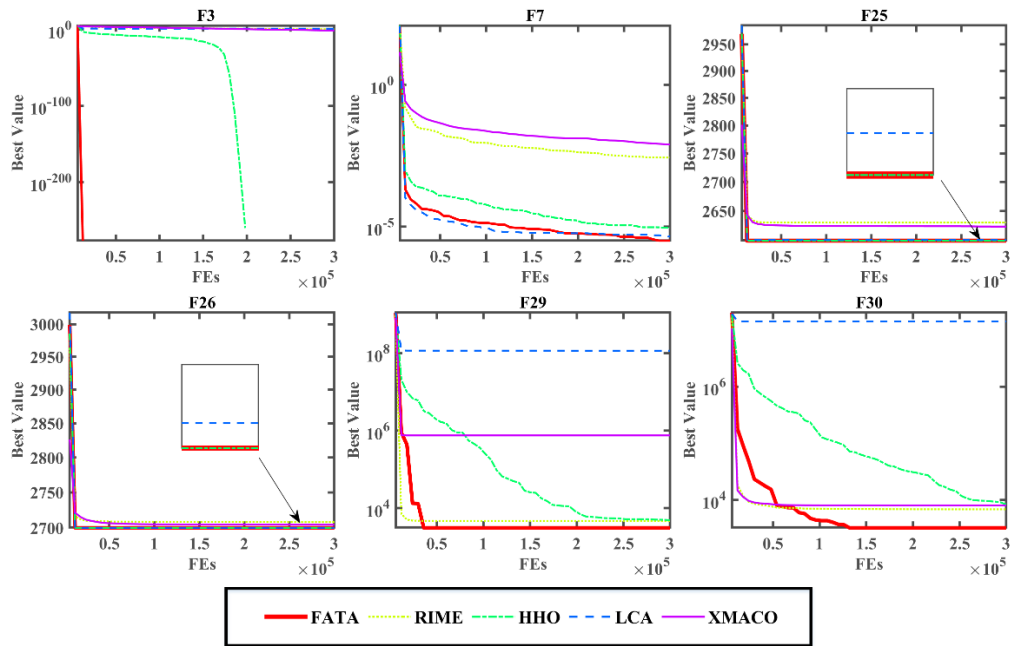


Figure 16. Comparisons between FATA and SOTA counterparts

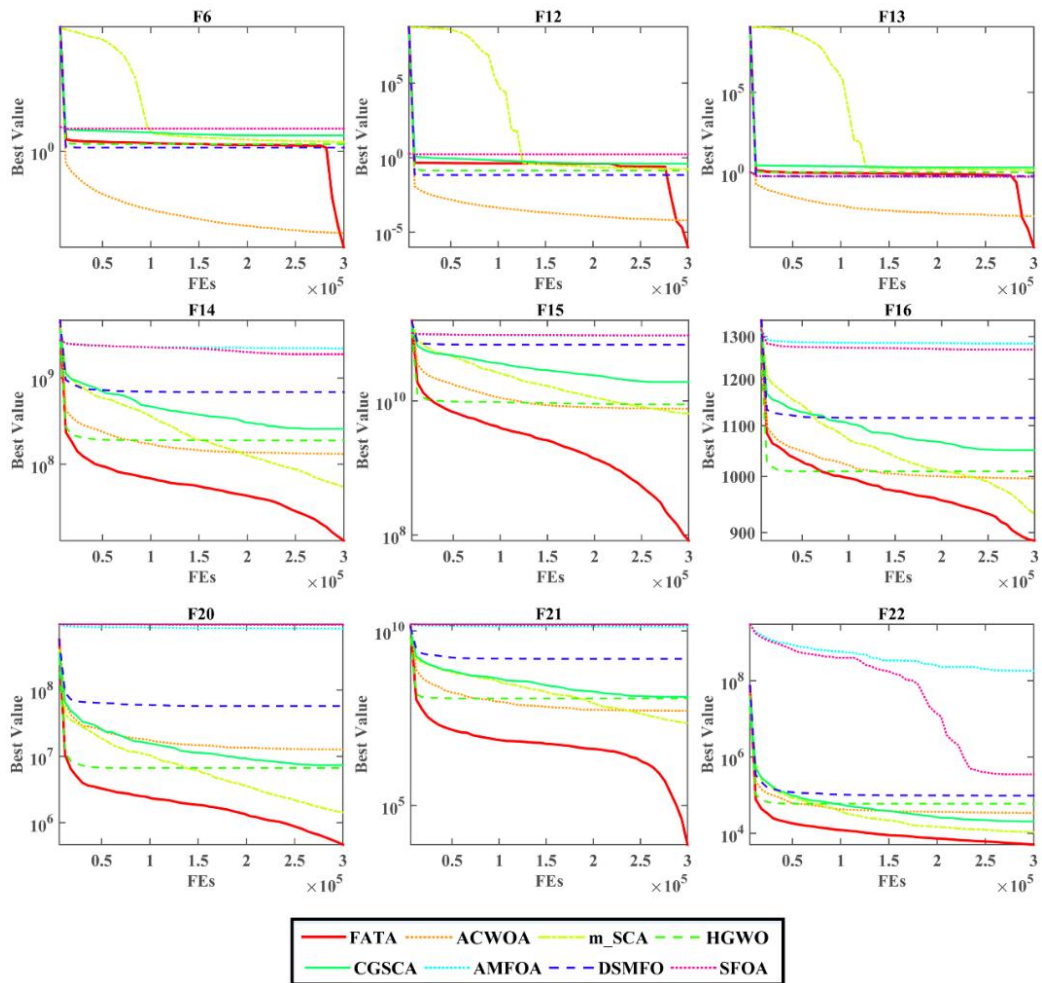


Figure 17. Comparisons between FATA and improved counterparts

4.10 Analysis of computational cost for FATA

To test the computational efficiency of the algorithm, this section designs optimization time cost experiments between FATA and comparative algorithms. The experimental results are subjected to statistical analysis and presented in bar charts. To provide a more intuitive comparison of the time cost between the FATA and different types of algorithms, two sets of experiments of the same type are conducted in this section.

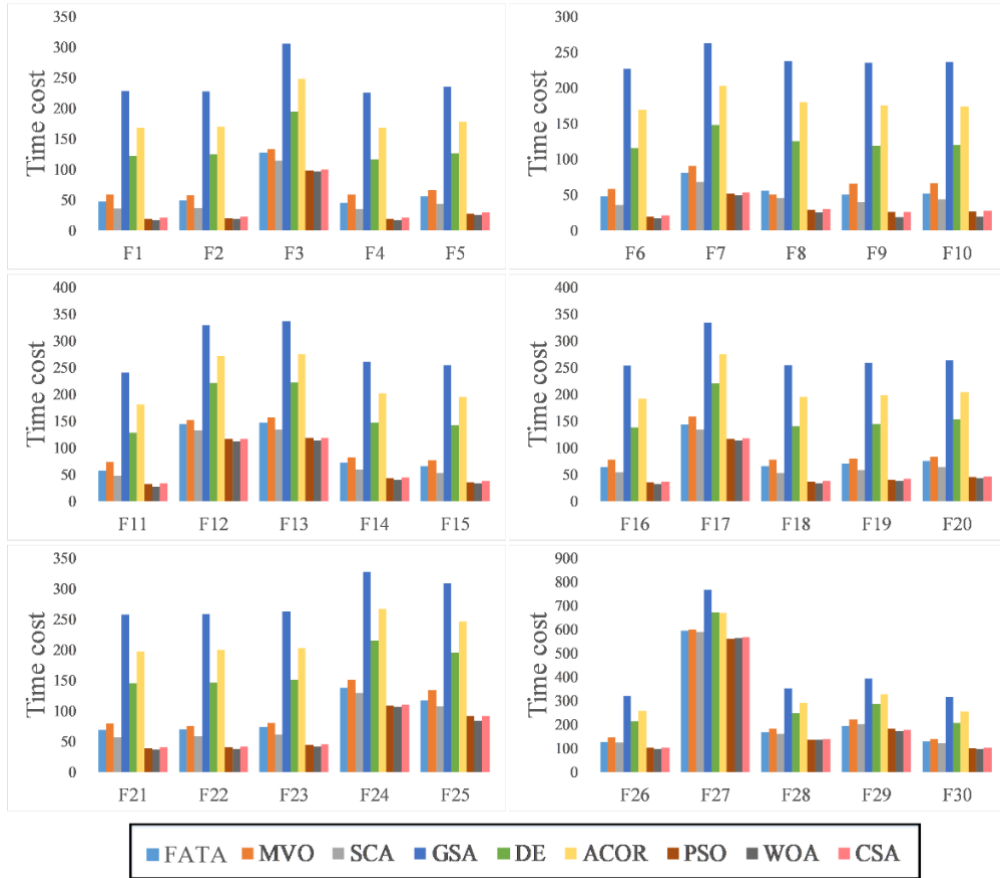


Figure 18. The computational cost of FATA with classical algorithm

Figures 18 and 19 visualize the results of the experimental analysis of the computational cost of FATA. Tables A.12, A.13 and A.14 show the results of the computational cost data for this experiment. Furthermore, the results in the table are counted in seconds. Among them, the computational cost of AOA on the function is too large, which is not shown in the figure. Figure 18 shows that FATA consumes less cost than MVO, GSA, AOA, DE, and ACOR on the function set. Although the time difference between FATA and SCA, PSO, WOA, and CSA is within 35 seconds for some functions, the computational cost of FATA is competitive when combined with the optimal solution of FATA on the function set.

Furthermore, in order to provide a more intuitive representation of the computational cost differences between all the algorithms, the computational cost of the LCA, which is too high, is reduced to one-third of its original value in Figure 19. Based on the analysis results in Figure 19, FATA demonstrates similar time expenditure to RIME and HHO but achieves better time performance compared to other SOTA algorithms. Additionally, FATA is able to obtain superior computational results within a reasonable amount of time. The figure illustrates that FATA incurs lower computational costs than XMACO, LCA, HGWO, CGSCA, and DSMFO in the function set. So, the computational cost of FATA is competitive on some functions when combined with the optimal solution of FATA in the function set.

The experimental results from the two graphs clearly indicate that FATA requires less time

compared to other comparative algorithms when dealing with both unimodal functions and multimodal functions. Additionally, it can be observed that the FATA algorithm spends more optimization time when facing hybrid/composition functions (F21–F30) compared to other types of functions. This suggests that the mirage light filtering principle and the light propagation principle in the algorithm continuously balance the global exploration and local exploitation capabilities, resulting in more time consumption during the optimization process. However, based on these two sets of experiments on time consumption, the FATA algorithm demonstrates more comprehensive efficiency in handling multiple types of function sets compared to other algorithms.

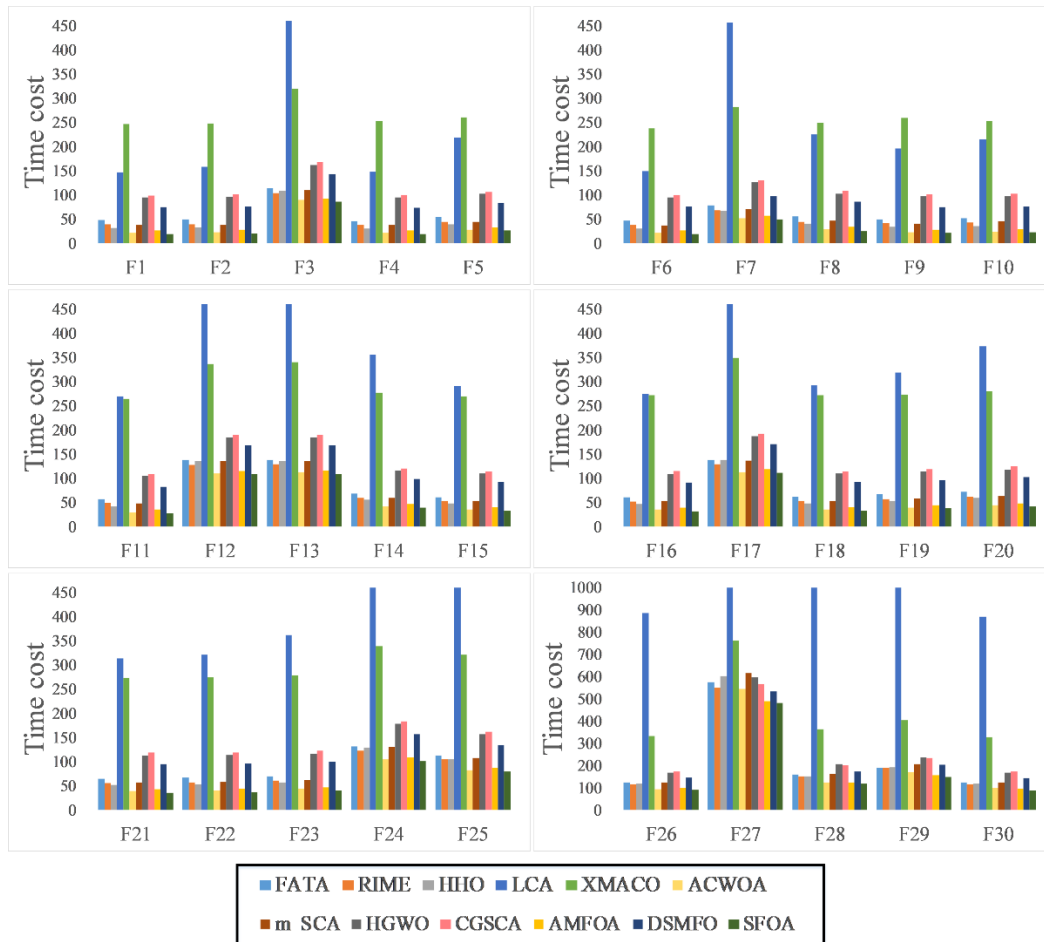


Figure 19. The computational cost of FATA with classical algorithm

5 Application to engineering optimization

Most real optimization problems have constraints in the design process and optimizing their feature space needs strong performance that can find optimal solutions with respect to constraints [67, 68]. Among them, the engineering design problem comprises the objective function and the constraints. The process of considering control variables, equations or inequalities, and linear or nonlinear constraints in an engineering problem is called the constraint process. Traditional

engineering optimization methods usually use linear programming models to solve them, so the optimal solution is poor and inefficient. In recent years, swarm intelligence algorithms have gradually become the most popular optimization methods in the field, with the potential to solve these problems.

This section applies the FATA to three widely used engineering design problems: welded beam design, pressure vessel design, and cantilever structure design.

5.1 The welded beam design problem

The goal of the welded beam design problem is to minimize the design cost. In Table 14, the constraint variables of the issue include deflection (δ), shear stress (τ), bucking load (P_c), and bending stress (θ). Meanwhile, welding joint length (l), beam thickness (b), beam width (t), and welding seam thickness (h) are the four relational variables in the problem. Figure 20 shows the structure of the welded beam project. The mathematical model for the problem is shown below (Eqs. (18-20)).

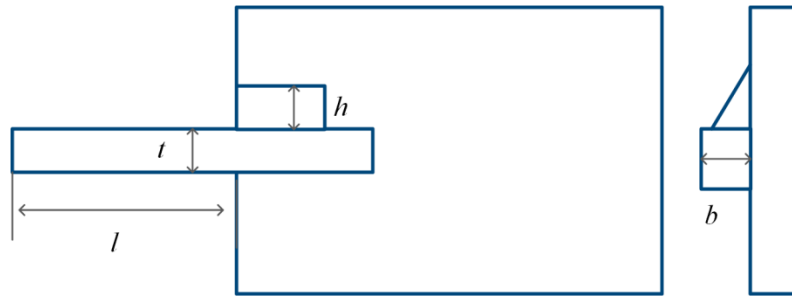


Figure 20. Structure of welded beam design

Consider: $X = [x_1, x_2, x_3, x_4] = [h, l, t, b]$ (18)

Minimize: $f(X) = 1.10471 \times x_1^2 + 0.04811 \times x_3 x_4 (14 + x_4)$ (19)

$$g_1(X) = \tau(X) - \tau_{max} \leq 0$$

$$g_2(X) = \sigma(X) - \sigma_{max} \leq 0$$

$$g_3(X) = \delta(X) - \delta_{max} \leq 0$$

$$g_4(X) = x_1 - x_4 \leq 0$$

Subject to: $g_5(X) = P - P_c(X) \leq 0$ (20)

$$g_6(X) = 0.125 - x_1 \leq 0$$

$$g_7(X) = 1.10471 \times x_1^2 + 0.04811 \times x_3 x_4 (14 + x_2) - 5.0 \leq 0$$

$$0.1 \leq x_1, x_4 \leq 2$$

$$0.1 \leq x_2, x_3 \leq 10$$

Table 14 The parameter set of the model

Parameter		
$\tau(X) = \sqrt{(\tau')^2 + 2\tau'\tau'' \frac{x_2}{2R} + (\tau'')^2}$	$\tau' = \frac{P}{\sqrt{2}x_1x_2}$	$P = 60001b$

$$\begin{aligned}
J &= 2 \left\{ \sqrt{2}x_1x_2 \left[\frac{x_2^2}{4} + \left(\frac{x_1 + x_3}{2} \right)^2 \right] \right\} & \tau'' &= \frac{MR}{J} & L &= 14 \text{ in} \dots \delta_{max} \\
& & & & &= 0.25 \text{ in} \cdot E \\
R &= \sqrt{\frac{x_2^2}{4} + \left(\frac{x_1 + x_3}{2} \right)^2} & M &= P \left(L + \frac{x_2}{2} \right) & E &= 30 \times 10^6 \text{ psi} \\
P_c(X) &= \frac{4.013E \sqrt{\frac{x_3^2 x_4^6}{36}}}{L^2} \left(1 - \frac{x_3}{2L} \sqrt{\frac{E}{4G}} \right) & \delta(X) &= \frac{6PL^3}{Ex_3^2 x_4} & G &= 12 \times 10^6 \text{ psi} \\
\sigma_{max} &= 30000 \text{ psi} & \sigma(X) &= \frac{6PL}{x_4 x_3^2} & \tau_{max} &= 13600 \text{ psi}
\end{aligned}$$

Table 15 shows the optimization results obtained by FATA, WCA, IHS, CDE, GWO, NDE, WOA, and GSA for this problem. The values of the constraint variables obtained by FATA are $h = 0.1885$, $l = 3.4905$, $t = 9.0947$, $b = 0.2069$. The optimum cost obtained by FATA is 1.720001. The proposed method has a smaller cost than other comparative algorithms.

Table 15 The results of this experiment

Algorithm	Optimal values for variables				Optimum cost
	h	l	t	b	
FATA	0.188500	3.490500	9.094700	0.206900	1.720001
WCA [69]	0.205728	3.470522	9.036620	0.205729	1.724856
IHS [70]	0.20573	3.47049	9.03662	0.20573	1.7248
CDE[71]	0.203137	3.542998	9.033498	0.206179	1.733462
GWO[30]	0.205700	3.478400	9.036800	0.205800	1.726240
NDE[72]	0.205729	3.470488	9.903662	0.205729	1.724852
WOA[31]	0.2054	3.4843	9.0374	0.2063	1.73050
GSA[51]	0.182129	3.856979	10.00000	0.202376	1.879950

5.2 The pressure vessel design problem

Pressure vessel design engineering is designed to minimize the cost of materials used in the project. The variables in the problem are the inner radius (R), the head thickness (T_h), the shell thickness (T_s), and the section range minus head (L). Figure 21 shows the 3D model of the pressure vessel. The mathematical model for the problem is shown below (Eqs. (21-23)).

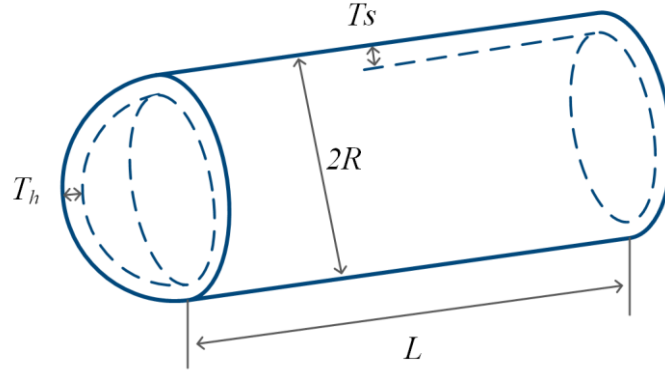


Figure 21. Structure of pressure vessel design

Consider: $X = [x_1, x_2, x_3, x_4] = [T_s, T_h, R, L]$ (21)

Minimize: $f(X) = 0.6224 \times x_1 x_3 x_4 + 1.7781 \times x_3 x_1^2 + 3.1661 \times x_4 x_1^2 + 19.84 \times x_3 x_1^2$ (22)

$$g_1(X) = -x_1 + 0.0193 \times x_3 \leq 0$$

$$g_2(X) = -x_3 + 0.00954 \times x_3 \leq 0$$

Subject to: $g_3(X) = -\pi \times x_4 x_3^2 - \frac{4}{3} \times \pi \times x_3^3 + 1296000 \leq 0$ (23)

$$g_4(X) = x_4 - 240 \leq 0$$

$$0 \leq x_1, x_2 \leq 99$$

$$10 \leq x_3, x_4 \leq 200$$

Table 16 shows the optimization results obtained by FATA, AGOA, GSA, EWOA, GA, CPSO, and Branch-bound for this problem. The values of the constraint variables obtained by FATA are $T_s = 0.8125$, $T_h = 0.4375$, $R = 42.09363$, and $L = 176.7089$. The optimum cost obtained by FATA is 6060.59696. FATA obtains the best optimization results.

Table 16 The results of this experiment

Algorithm	Optimal values for variables				Optimum cost
	T_s	T_h	R	L	
FATA	0.812500	0.437500	42.09363	176.7089	6060.59696
AGOA[73]	0.87500	0.437500	45.19610	142.7458	6135.11600
GSA [51]	1.12500	0.62500	55.98866	84.45203	8538.83590
EWOA[10]	0.901034	0.452897	46.67809	127.0967	6160.20900
GA[74]	0.937500	0.500000	48.32900	112.6790	6410.38100
CPSO[75]	0.812500	0.437500	42.09120	176.7465	6061.07770
Branch-bound[76]	1.1250	0.6250	47.7000	117.7010	8129.10360

5.3 The cantilever structure design problem

As shown in Figure 22, the cantilever structure consists of five hollow square sections. The cantilever structure design problem aims to minimize engineering mass. The constraint variable for

this problem is to calculate the heights of five box types, x_1, x_2, x_3, x_4, x_5 , respectively. The mathematical model for the problem is shown below (Eqs. (24-26)).

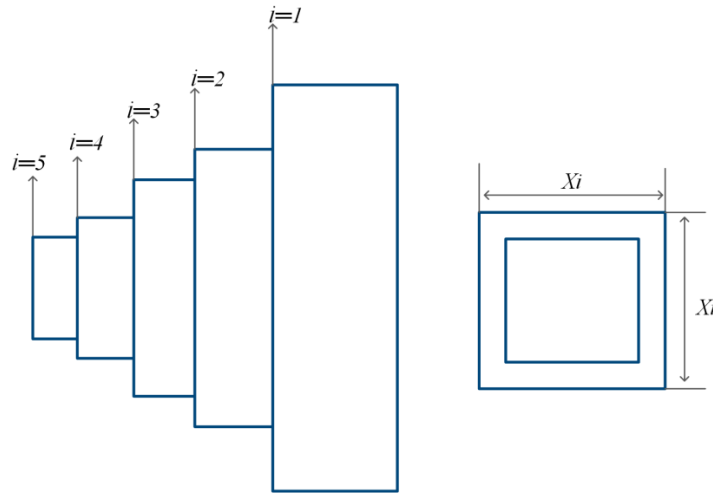


Figure 22. Structure of cantilever structure design

Consider: $X = [x_1, x_2, x_3, x_4, x_5]$ (24)

Minimize: $f(X) = 0.6224 \times (x_1 + x_2 + x_3 + x_4 + x_5)$ (25)

Subject to: $g(X) = \frac{61}{x_1^3} + \frac{37}{x_2^3} + \frac{19}{x_3^3} + \frac{7}{x_4^3} + \frac{1}{x_5^3} \leq 1$ (26)

$0.01 \leq x_1, x_2, x_3, x_4, x_5 \leq 100$

Table 17 shows the optimization results obtained by FATA, SMA, MMA, SOS, MFO, GCA, and CS for this problem. The values of the constraint variables obtained by FATA are $x_1 = 6.023555$, $x_2 = 5.298319$, $x_3 = 4.499286$, $x_4 = 3.502969$, and $x_5 = 2.149635$. The optimum value obtained by FATA is 1.33996. The proposed method has a smaller cost.

Table 17 The results of this experiment

Algorithm	Optimal values for variables					Optimum
	x_1	x_2	x_3	x_4	x_5	
FATA	6.023555	5.298319	4.499286	3.502969	2.149635	1.33996
SMA[77]	6.017757	5.310892	4.493758	3.501106	2.161600	1.33996
MMA	6.0100	5.3000	4.4900	3.4900	2.1500	1.3400
SOS[78]	6.0188	5.3034	4.495900	3.4990	2.1556	1.33996
MFO[19]	5.9830	5.3167	4.4973	3.5136	2.1616	1.33998
GCA[79]	6.0100	5.3000	4.4900	3.4900	2.1500	1.3400
CS[80]	6.0089	5.3049	4.5023	3.5077	2.1504	1.3999

6 Discussion

This paper proposes a new FATA morgana algorithm based on the phenomenon of mirage to solve multi-type continuous optimization problems. The algorithm simulates the formation process of a mirage. When facing multi-type continuous optimization functions, FATA achieves better optimization accuracy and stability in handling unimodal functions and hybrid/composition functions compared to multimodal functions. However, the FATA consumes more time handling hybrid/composition functions than other functions. Overall, considering the performance of the FATA on multi-type continuous function sets in terms of solution accuracy, stability, and computation time, it exhibits more comprehensive performance than many excellent SOTAs. Furthermore, when solving engineering design problems, the FATA demonstrates high efficiency in solving single-objective, non-differentiable problems and can handle engineering problems with multiple constraints. However, the limitation of the algorithm is that further optimization is needed when addressing multi-objective research problems.

Therefore, while the FATA presented in this paper is designed for single-objective continuous optimization problems, its scalability needs to be further explored and researched when it comes to multi-objective optimization problems, which are also common in real-world engineering problems. In the study of multi-objective optimization problems based on the Pareto optimal solution set, the FATA retains the flexibility to further adjust the structure of the optimization objective functions. Therefore, objective functions based on the Pareto optimal solution set can be adaptively combined with the FATA. Furthermore, the population encoding for the multi-objective FATA can also transition from the adaptability of the single-objective population. When facing multi-objective optimization problems, the population will contain more information. In this regard, the strategies of the mirage light filtering principle and the light propagation principle in the FATA can consider diffusing the principles of calculus into the iterative computation of the population to adapt to multi-objective optimization problems.

Therefore, the design of optimization objective functions based on the Pareto optimal solution set in the multi-objective FATA algorithm, as well as the multi-objective population update strategy of the mirage light filtering principle and the light propagation principle in the FATA, are the core technologies for further optimizing the FATA.

7 Conclusions and future directions

This work proposes a new physics-based fata morgana algorithm to solve multi-type continuous optimization problems. The proposed algorithm simulates the process of mirage formation. FATA designs the mirage light filtering principle and the light propagation strategy. The former is employed to design the population search strategy, while the latter is used to construct the individual search strategy. The MLF is an algorithmic population search strategy incorporating the theory of definite integration. The trigonometric principle is combined with the individual search strategy known as LPS. These two search strategies can more effectively balance FATA exploitation and exploration.

To analyze the performance of the FATA, some experiments are used for FATA testing. The qualitative analysis experiment demonstrates the optimization rules and characteristics of the Fata morgana algorithm. The algorithm's search strategies and the population distribution allow it to have good convergence speed and avoid premature convergence. Then, the analysis of exploitation ability, exploration ability, and ability to escape from local optimum demonstrate the multi-faceted optimization capability of the fata morgana algorithm more visually. Furthermore, FATA was compared with recent state-of-the-art (SOTA) algorithms in multi-type function optimization experiments. The strengths and weaknesses of the FATA algorithm for different types of functions were analyzed. In conclusion, the FATA algorithm achieved more comprehensive performance in handling various functions. Moreover, the computational cost experiment results also indicate the algorithm's competitiveness in terms of solving time.

In addition, the proposed algorithm has good convergence speed and optimal solutions for solving multi-type continuous functions. The fata morgana algorithm is compared with a broad array of competitive optimizers on benchmark functions and three classical engineering design problems to evaluate its performance. First, the experimental results demonstrate the comprehensiveness and competitiveness of FATA. Then, the algorithm obtains better results than its counterparts in engineering problems. Moreover, FATA has excellent potential to be used as an efficient computer-aided tool for dealing with practical optimization tasks. In the future, the fata morgana algorithm can be combined with other methods as an effective tool for practical engineering design tasks, neural architecture search problems, and multi-objective solution problems. Meanwhile, the fata morgana algorithm will be applied to medical, economics, and primary science fields, including economic scheduling problems, medical image segmentation, etc.

Acknowledgement

This work was supported in part by the Natural Science Foundation of Zhejiang Province (LZ22F020005), National Natural Science Foundation of China (62076185, 62301367), Natural Science Foundation of Jilin Province (YDZJ202201ZYTS567). We acknowledge the comments of the reviewers.

Appendix A

Table. A.1 Results on the unimodal functions with improved algorithms

	F1		F2		F3	
	AVG	STD	AVG	STD	AVG	STD
FATA	0.0000E+00	0.0000E+00	4.0829E-204	0.0000E+00	0.0000E+00	0.0000E+00
ACWOA	0.0000E+00	0.0000E+00	0.0000E+00	0.0000E+00	0.0000E+00	0.0000E+00
m_SCA	0.0000E+00	0.0000E+00	1.0987E-312	0.0000E+00	4.0740E-205	0.0000E+00
HGWO	8.9366E-106	4.8948E-105	3.5756E-78	1.9584E-77	9.4232E-116	3.6315E-115
CGSCA	0.0000E+00	0.0000E+00	0.0000E+00	0.0000E+00	0.0000E+00	0.0000E+00
AMFOA	3.2156E-09	1.8296E-09	2.8224E-04	7.4997E-05	1.0108E-06	5.8072E-07
DSMFO	0.0000E+00	0.0000E+00	0.0000E+00	0.0000E+00	0.0000E+00	0.0000E+00
SFOA	1.0014E-08	3.9718E-11	5.4809E-04	1.2031E-06	3.1578E-06	1.0286E-08
	F4		F5		F6	
	AVG	STD	AVG	STD	AVG	STD
FATA	6.5084E-04	7.6474E-04	4.2255E-02	5.7934E-02	1.8031E-04	1.3376E-04
ACWOA	0.0000E+00	0.0000E+00	2.5210E+01	1.8297E-01	6.4111E-04	2.1318E-04
m_SCA	1.9478E-161	1.0669E-160	2.7271E+01	9.5198E-01	2.3143E+00	6.2040E-01
HGWO	3.4697E-79	8.3572E-79	2.7216E+01	2.4187E-01	1.8686E+00	2.0957E-01
CGSCA	1.7323E-293	0.0000E+00	2.7493E+01	7.4079E-01	4.1003E+00	2.4814E-01
AMFOA	1.2318E-05	2.5026E-06	2.8191E+01	2.8350E-01	7.5003E+00	7.5246E-05
DSMFO	0.0000E+00	0.0000E+00	2.8420E+01	2.1782E-01	1.3810E+00	6.3009E-01
SFOA	1.8266E-05	3.5350E-08	2.8707E+01	1.0965E-04	7.5005E+00	1.3250E-06
	F7		F14		F15	
	AVG	STD	AVG	STD	AVG	STD
FATA	2.3561E-05	1.5679E-05	1.2963E+07	6.2371E+06	8.2344E+07	3.3756E+07
ACWOA	5.2924E-06	4.8227E-06	1.3154E+08	5.2253E+07	7.6155E+09	3.3067E+09
m_SCA	8.7051E-05	7.9434E-05	5.4404E+07	2.5820E+07	6.4477E+09	3.2394E+09
HGWO	4.0148E-06	4.0569E-06	1.8832E+08	5.4369E+07	8.8281E+09	1.7560E+09
CGSCA	3.6164E-05	4.2374E-05	2.5670E+08	5.5558E+07	1.9145E+10	3.5775E+09
AMFOA	2.9621E-05	2.1821E-05	2.2042E+09	1.4710E+08	9.3268E+10	1.1510E+09
DSMFO	5.8361E-06	5.7066E-06	6.8976E+08	2.4857E+08	6.8665E+10	1.4264E+10
SFOA	4.3599E-05	2.0426E-05	1.8964E+09	7.7742E+07	9.4740E+10	4.6632E+09

Table. A.2 The statistical results of FATA versus other original peers

	MVO	SCA	AOA
F1	0.0000017344	0.0000017344	1.0000000000
F2	0.0000017344	0.0000017344	0.0000017344
F3	0.0000017344	0.0000017344	1.0000000000
F4	0.0000017344	0.0218267216	0.0000017344
F5	0.0000017344	0.0000017344	0.0000017344
F6	0.0000017344	0.0000017344	0.0000017344
F7	0.0000017344	0.0000017344	0.0000017344
F14	0.0000023534	0.0000017344	0.0000017344
F15	0.0000017344	0.0000017344	0.0000017344
	GSA	DE	ACOR
F1	0.0000017344	0.0000017344	0.0000017344
F2	0.0000017344	0.0000017344	0.0000017344
F3	0.0000017344	0.0000017344	0.0000017127
F4	0.0000017344	0.0000017344	0.0000017344
F5	0.0000017344	0.0000017344	0.0000023534
F6	0.0000017344	0.0000017344	0.0000017344
F7	0.0000017344	0.0000017344	0.0000017344
F14	0.0000017344	0.0001604638	0.0000311232
F15	0.0000017344	0.0000017344	0.0000311232
	PSO	WOA	CSA
F1	0.0000017344	1.0000000000	0.0000017344
F2	0.0000017344	0.0000017344	0.0000017344
F3	0.0000017344	0.0000017344	0.0000017344
F4	0.0000017344	0.0006639213	0.0000017344
F5	0.0000017344	0.0000017344	0.0000017344
F6	0.0000017344	0.0000023534	0.0000017344
F7	0.0000017344	0.0001604638	0.0000017344
F14	0.0195692152	0.0000021266	0.0000017344
F15	0.0001056950	0.0000023534	0.0000017344

Table. A.3 The statistical results of FATA versus other improved peers

	ACWOA	m_SCA	HGWO	CGSCA
F1	1.0000000000	1.0000000000	0.0000017344	1.0000000000
F2	0.0000017344	0.0000017344	0.0000017344	0.0000017344
F3	1.0000000000	0.0000017344	0.0000017344	1.0000000000
F4	0.0000017344	0.0000017344	0.0000017344	0.0000017344
F5	0.0000017344	0.0000017344	0.0000017344	0.0000017344
F6	0.0000017344	0.0000017344	0.0000017344	0.0000017344
F7	0.0000035152	0.0001250568	0.0000076909	0.2210215748
F14	0.0000017344	0.0000026033	0.0000017344	0.0000017344
F15	0.0000017344	0.0000017344	0.0000017344	0.0000017344
	AMFOA	DSMFO	SFOA	
F1	0.0000017344	1.0000000000	0.0000017344	

F2	0.0000017344	0.0000017344	0.0000017344
F3	0.0000017344	1.0000000000	0.0000017344
F4	0.0000017344	0.0000017344	0.0000019209
F5	0.0000017344	0.0000017344	0.0000017344
F6	0.0000017344	0.0000017344	0.0000017344
F7	0.2369361866	0.0000093157	0.0001890972
F14	0.0000017344	0.0000017344	0.0000017344
F15	0.0000017344	0.0000017344	0.0000017344

Table. A.4 Comparison results on the multimodal functions with improved algorithms

Function	F8		F9	
	AVG	STD	AVG	STD
FATA	-1.2569E+04	2.6084E-04	0.0000E+00	0.0000E+00
ACWOA	-1.2569E+04	1.1782E-03	0.0000E+00	0.0000E+00
m_SCA	-6.8445E+03	6.8560E+02	0.0000E+00	0.0000E+00
HGWO	-5.2585E+03	7.6553E+02	0.0000E+00	0.0000E+00
CGSCA	-4.6916E+03	4.5036E+02	0.0000E+00	0.0000E+00
AMFOA	-1.9551E+02	7.5718E+01	5.3702E-07	3.0874E-07
DSMFO	-1.2569E+04	6.2917E-02	0.0000E+00	0.0000E+00
SFOA	-3.4352E+03	4.5921E+03	1.9881E-06	7.4923E-09
Function	F10		F11	
	AVG	STD	AVG	STD
FATA	3.8833E-04	5.6500E-04	0.0000E+00	0.0000E+00
ACWOA	1.1250E-15	9.0135E-16	0.0000E+00	0.0000E+00
m_SCA	4.6639E+00	8.5986E+00	0.0000E+00	0.0000E+00
HGWO	8.8818E-16	0.0000E+00	0.0000E+00	0.0000E+00
CGSCA	8.8818E-16	0.0000E+00	0.0000E+00	0.0000E+00
AMFOA	3.7624E-05	1.0010E-05	2.0150E-10	1.2142E-10
DSMFO	8.8818E-16	0.0000E+00	0.0000E+00	0.0000E+00
SFOA	7.3127E-05	1.5542E-07	6.6899E-10	2.6076E-12
Function	F12		F13	
	AVG	STD	AVG	STD
FATA	9.8054E-07	6.6361E-07	2.4815E-05	1.7108E-05
ACWOA	6.2226E-05	1.9520E-05	2.1038E-03	3.6926E-03
m_SCA	1.7941E-01	9.5167E-02	1.5096E+00	2.0266E-01
HGWO	1.3591E-01	3.0187E-02	1.1155E+00	1.2839E-01
CGSCA	3.9703E-01	4.1686E-02	2.1837E+00	9.9150E-02
AMFOA	1.6690E+00	1.0999E-05	5.8223E-01	1.0846E-01
DSMFO	6.9060E-02	4.5181E-02	6.4846E-01	2.3504E-01
SFOA	1.6691E+00	1.3791E-07	5.9622E-01	7.2892E-02
Function	F16		F17	
	AVG	STD	AVG	STD
FATA	8.8660E+02	1.1306E+01	1.2018E+03	4.9859E-01
ACWOA	9.9646E+02	3.0121E+01	1.2016E+03	4.8692E-01
m_SCA	9.3185E+02	2.5639E+01	1.2008E+03	4.7449E-01

HGWO	1.0096E+03	1.0790E+01	1.2014E+03	3.4592E-01
CGSCA	1.0505E+03	1.6004E+01	1.2025E+03	2.7039E-01
AMFOA	1.2832E+03	1.4467E+01	1.2079E+03	6.7803E-01
DSMFO	1.1162E+03	3.2646E+01	1.2028E+03	5.1871E-01
SFOA	1.2688E+03	1.0560E+01	1.2082E+03	3.3372E-06
Function	F18		F19	
Item	AVG	STD	AVG	STD
FATA	1.4005E+03	3.5358E-01	1.5629E+03	2.3444E+01
ACWOA	1.4213E+03	1.4504E+01	1.9507E+03	5.2857E+02
m_SCA	1.4129E+03	7.9989E+00	2.5001E+03	2.0154E+03
HGWO	1.4221E+03	3.8375E+00	2.0722E+03	8.2477E+02
CGSCA	1.4536E+03	9.7773E+00	7.7169E+03	4.8712E+03
AMFOA	1.7377E+03	1.1825E+01	5.8292E+05	4.3632E+04
DSMFO	1.5498E+03	4.1676E+01	1.0067E+05	8.8899E+04
SFOA	1.7103E+03	6.6320E+00	5.2721E+05	4.7724E+04

Table. A.5 The statistical results of FATA versus other original peers

	MVO	SCA	AOA
F8	0.0000017344	0.0000017344	0.0000017344
F9	0.0000017344	0.0625000000	1.0000000000
F10	0.0000017344	0.0001353608	0.0000023628
F11	0.0000017344	0.5000000000	0.5000000000
F12	0.0000017344	0.0000017344	0.0000017344
F13	0.0000017344	0.0000017344	0.0000017344
F16	0.0195692152	0.0000017344	0.0000017344
F17	0.0000017344	0.0000112654	0.0000017344
F18	0.3086148505	0.0000017344	0.0000017344
F19	0.0000017344	0.0000017344	0.0000017344
	GSA	DE	ACOR
F8	0.0000017344	0.0001149922	0.0000017344
F9	0.0000017344	1.0000000000	0.0000017322
F10	0.0000017344	0.0004216366	0.4171679331
F11	0.0000017344	1.0000000000	0.0000591118
F12	0.0000017344	0.0000017344	0.2058882231
F13	0.0000017344	0.0000017344	0.0471617472
F16	0.0000017344	0.0000017344	0.0000057517
F17	0.0000017344	0.0000026033	0.0000216302
F18	0.0407023114	0.0387230265	0.1588554993
F19	0.0000017344	0.0000017344	0.0000444934
	PSO	WOA	CSA
F8	0.0000017344	0.0001149922	0.0000017344
F9	0.0000017344	1.0000000000	0.0000017322
F10	0.0000017344	0.0004216366	0.4171679331
F11	0.0000017344	1.0000000000	0.0000591118
F12	0.0000017344	0.0000017344	0.2058882231

F13	0.0000017344	0.0000017344	0.0471617472
F16	0.0000017344	0.0000017344	0.0000057517
F17	0.0000017344	0.0000026033	0.0000216302
F18	0.0407023114	0.0387230265	0.1588554993
F19	0.0000017344	0.0000017344	0.0000444934

Table. A.6 The statistical results of FATA versus other improved peers

	ACWOA	m_SCA	HGWO	CGSCA
F8	0.0012866311	0.0000017344	0.0000017344	0.0000017344
F9	1.0000000000	1.0000000000	1.0000000000	1.0000000000
F10	0.0000022060	0.5428958259	0.0000022060	0.0000022060
F11	1.0000000000	1.0000000000	1.0000000000	1.0000000000
F12	0.0000017344	0.0000017344	0.0000017344	0.0000017344
F13	0.0000017344	0.0000017344	0.0000017344	0.0000017344
F16	0.0000017344	0.0000038822	0.0000017344	0.0000017344
F17	0.0270291566	0.0000035152	0.0003881114	0.0000047292
F18	0.0000017344	0.0000076909	0.0000017344	0.0000017344
F19	0.0000019209	0.0000237045	0.0000017344	0.0000017344
	AMFOA	DSMFO	SFOA	
F8	0.0000017344	0.0000057517	0.0000311232	
F9	0.0000017344	1.0000000000	0.0000017344	
F10	0.0175183936	0.0000022060	0.0387230265	
F11	0.0000017344	1.0000000000	0.0000017344	
F12	0.0000017344	0.0000017344	0.0000017344	
F13	0.0000017344	0.0000017344	0.0000017344	
F16	0.0000017344	0.0000017344	0.0000017344	
F17	0.0000017344	0.0000076909	0.0000017344	
F18	0.0000017344	0.0000017344	0.0000017344	
F19	0.0000017344	0.0000017344	0.0000017344	

Table. A.7 Comparison results on the hybrid and composite functions with improved algorithms

Item	F20		F21		F22	
	AVG	STD	AVG	STD	AVG	STD
FATA	4.6761E+05	3.3204E+05	7.5329E+03	3.2330E+03	5.0545E+03	3.3771E+03
ACWOA	1.2696E+07	1.1865E+07	5.1385E+07	4.0575E+07	3.4200E+04	1.2669E+04
m_SCA	1.4275E+06	1.8320E+06	2.2638E+07	3.1675E+07	1.0675E+04	5.7788E+03
HGWO	6.6893E+06	3.9000E+06	1.1640E+08	3.6699E+07	5.9838E+04	2.2938E+04
CGSCA	7.3758E+06	2.7892E+06	1.3000E+08	7.1208E+07	2.0522E+04	1.0941E+04
AMFOA	8.4384E+08	1.7006E+08	1.3011E+10	2.6805E+08	1.8274E+08	2.5165E+08
DSMFO	5.7407E+07	3.9710E+07	1.5749E+09	1.4604E+09	9.7468E+04	8.4128E+04
SFOA	9.6682E+08	7.0003E+07	1.4988E+10	1.0700E+09	3.5268E+05	4.2156E+04
Item	F23		F24		F25	
	AVG	STD	AVG	STD	AVG	STD
FATA	4.4545E+05	3.0265E+05	2.5000E+03	1.1942E-13	2.6000E+03	3.3253E-04
ACWOA	4.9776E+06	3.7472E+06	2.5250E+03	6.5139E+01	2.6000E+03	1.9225E-05
m_SCA	4.9805E+05	4.6432E+05	2.6391E+03	1.0228E+01	2.6000E+03	9.2412E-04

HGWO	1.9406E+06	1.0616E+06	2.5106E+03	4.1010E+01	2.6000E+03	0.0000E+00
CGSCA	1.7758E+06	1.2979E+06	2.5000E+03	0.0000E+00	2.6000E+03	1.7629E-06
AMFOA	7.8753E+08	3.3224E+08	2.5000E+03	4.2077E-04	2.6000E+03	2.3652E-03
DSMFO	2.0935E+07	1.5064E+07	2.5000E+03	0.0000E+00	2.6000E+03	0.0000E+00
SFOA	2.6431E+08	5.0385E+07	2.5000E+03	5.3808E-06	2.6000E+03	2.4358E-05
	F26		F27		F28	
Item	AVG	STD	AVG	STD	AVG	STD
FATA	2.7000E+03	4.3879E-13	2.9000E+03	6.8516E-03	3.0000E+03	1.2853E-02
ACWOA	2.7000E+03	0.0000E+00	3.5883E+03	3.3911E+02	3.6817E+03	1.0675E+03
m_SCA	2.7129E+03	3.6096E+00	3.1750E+03	1.4325E+02	3.8998E+03	1.5033E+02
HGWO	2.7000E+03	0.0000E+00	3.5918E+03	2.4273E+02	4.2206E+03	2.0210E+02
CGSCA	2.7000E+03	0.0000E+00	2.9000E+03	0.0000E+00	3.0000E+03	0.0000E+00
AMFOA	2.7000E+03	6.2505E-06	2.9000E+03	5.6337E-05	3.0000E+03	1.4697E-04
DSMFO	2.7000E+03	0.0000E+00	2.9000E+03	0.0000E+00	3.0000E+03	0.0000E+00
SFOA	2.7000E+03	6.5595E-08	2.9000E+03	7.0392E-07	3.0000E+03	1.9148E-06
	F29		F30			
Item	AVG	STD	AVG	STD		
FATA	1.3262E+04	2.1200E+04	6.2027E+03	5.3065E+03		
ACWOA	1.8902E+07	1.4975E+07	3.8939E+05	2.6077E+05		
m_SCA	1.2375E+06	3.9495E+06	4.7968E+04	2.3599E+04		
HGWO	3.2509E+06	3.3205E+06	3.2000E+03	6.3160E-05		
CGSCA	3.1000E+03	0.0000E+00	2.1439E+04	7.5827E+04		
AMFOA	4.6291E+03	3.7219E+02	3.3064E+03	2.7243E+01		
DSMFO	3.1000E+03	0.0000E+00	3.2000E+03	0.0000E+00		
SFOA	6.2002E+03	5.3286E+00	3.4112E+03	4.1091E-01		

Table. A.8 The statistical results of FATA versus other original peers

	MVO	SCA	AOA
F20	0.0000084661	0.0000017344	0.0000017344
F21	0.5999359282	0.0000017344	0.0000028786
F22	0.0000216302	0.0000052165	0.0000021266
F23	0.0000102463	0.0000069838	0.0000021266
F24	0.0000017344	0.0000017344	0.0001964367
F25	0.0000017344	0.0000017344	0.0000017344
F26	0.0000017344	0.0000017344	1.0000000000
F27	0.0000017344	0.0000017344	0.9753871642
F28	0.0000017344	0.0000017344	0.3146663266
F29	0.0004195510	0.0000017344	0.0000093157
F30	0.0687136308	0.0000017344	0.0000028786
	GSA	DE	ACOR
F20	0.0000237045	0.0000136011	0.0000035152
F21	0.0000311232	0.0519306650	0.0005706437
F22	0.0000017344	0.4284300285	0.0570964952
F23	0.0001477276	0.0719033301	0.0000023534
F24	0.0000017344	0.0000000432	0.0000011019

F25	0.0000017344	0.0000017344	0.0000017344
F26	0.0000017344	0.0000017344	0.0000017344
F27	0.0000017344	0.0000017344	0.0000017344
F28	0.0000017344	0.0000017344	0.0000017344
F29	0.0000891873	0.0124525604	0.0010356813
F30	0.0598356014	0.5304400912	0.0300098913
	PSO	WOA	CSA
F20	0.0004195510	0.0000017344	0.0000017344
F21	0.0000017344	0.0000631976	0.0000017344
F22	0.0000031817	0.0000019209	0.0000486026
F23	0.0005706437	0.0000237045	0.0000017344
F24	0.0000017344	0.0000017344	0.0000017344
F25	0.0000017344	0.0000017344	0.0000017344
F26	0.0000017344	0.0001318339	0.0000017344
F27	0.0000017344	0.0000017344	0.0000017344
F28	0.0000017344	0.0000019209	0.0000017344
F29	0.0300098913	0.0000047019	0.0022551239
F30	0.0000259671	0.0000017344	0.0001359477

Table. A.9 The statistical results of FATA versus other improved peers

	ACWOA	m_SCA	HGWO	CGSCA
F20	0.0000017344	0.0004195510	0.0000017344	0.0000017344
F21	0.0000017344	0.0000017344	0.0000017344	0.0000017344
F22	0.0000017344	0.0000891873	0.0000017344	0.0000019209
F23	0.0000019209	0.7970983030	0.0000023534	0.0000069838
F24	0.1250000000	0.0000017344	0.1250000000	1.0000000000
F25	0.0000017344	0.0092710252	0.0000017344	0.0000017344
F26	1.0000000000	0.0000025631	1.0000000000	1.0000000000
F27	0.0000017344	0.0000017344	0.0000031817	0.0000025631
F28	0.9753871642	0.0000017344	0.0000017344	0.0000017344
F29	0.0000035150	0.0000163945	0.0000631976	0.0009765625
F30	0.0000025631	0.0000017344	0.0022009063	0.0278570980
	AMFOA	DSMFO	SFOA	
F20	0.0000017344	0.0000017344	0.0000017344	
F21	0.0000017344	0.0000017344	0.0000017344	
F22	0.0000017344	0.0000017344	0.0000017344	
F23	0.0000017344	0.0000017344	0.0000017344	
F24	0.0000017344	1.0000000000	0.0000017344	
F25	0.0000017344	0.0000017344	0.0000017344	
F26	0.0000017344	1.0000000000	0.0000017344	
F27	0.0000123808	0.0000025631	0.0000530699	
F28	0.0000017344	0.0000017344	0.0000038822	
F29	0.4048347222	0.0009765625	0.6288430021	
F30	0.0471617472	0.0002930525	0.0977721901	

Table. A.10 The results of this experiment

	F1		F2		F3	
	AVG	STD	AVG	STD	AVG	STD
FATA	0.0000E+00	0.0000E+00	6.6957E-234	0.0000E+00	8.1682E-113	2.8945E-112
EPSO	3.0890E-36	7.2330E-36	2.7180E-44	1.4887E-43	1.7929E-68	9.8141E-68
ASCA_PSO	8.2447E+01	9.8882E+00	7.2857E-202	0.0000E+00	2.6786E-122	1.0959E-121
SCADE	0.0000E+00	0.0000E+00	5.7137E-23	6.8946E-23	7.7170E-24	4.1137E-23
SADE	5.9774E-154	2.0621E-153	4.2975E+01	4.1446E+00	0.0000E+00	0.0000E+00
MPEDE	2.1190E-224	0.0000E+00	0.0000E+00	0.0000E+00	4.4201E+02	2.5373E+02
LSHADE	9.2792E-199	0.0000E+00	5.8278E-105	2.3489E-104	2.0294E+02	3.8831E+01
	F4		F5		F6	
	AVG	STD	AVG	STD	AVG	STD
FATA	0.0000E+00	0.0000E+00	6.2412E-05	1.4822E-04	1.7331E-07	2.8344E-07
EPSO	2.2751E-05	6.2513E-05	3.6007E+00	2.1843E-01	4.1828E-02	6.9147E-02
ASCA_PSO	2.8974E-35	1.4766E-34	4.2168E-194	0.0000E+00	2.5063E+01	2.3739E+01
SCADE	1.9302E-49	9.8246E-49	3.9404E-03	2.0448E-02	6.4128E+04	1.3266E+04
SADE	1.1730E-38	2.6881E-38	7.0262E-05	1.7810E-04	1.1062E+01	1.3186E+01
MPEDE	5.4401E-09	2.9797E-08	1.9855E-04	2.7548E-04	1.7166E+01	1.6303E+01
LSHADE	7.1951E-04	7.5903E-04	4.2200E-08	1.1681E-07	1.4618E+00	1.9540E+00
	F7		F8		F9	
	AVG	STD	AVG	STD	AVG	STD
FATA	7.9733E-01	1.6219E+00	4.5195E-33	7.5365E-33	3.0641E+01	5.6674E+00
EPSO	7.9732E-01	1.6219E+00	6.1630E-33	7.6771E-33	2.5920E-04	1.4932E-04
ASCA_PSO	5.3633E-01	1.3765E+00	8.2173E-33	8.6529E-33	4.4373E-03	1.6423E-03
SCADE	1.5947E-04	1.5743E-04	0.0000E+00	0.0000E+00	2.6955E-03	1.3244E-03
SADE	5.8546E-29	2.3146E-29	1.0272E-34	5.6260E-34	7.2435E-03	4.6078E-03
MPEDE	8.1981E+01	8.6878E+00	3.5039E-05	3.3198E-05	3.4172E-03	1.2339E-03
LSHADE	2.0284E-07	1.5642E-07	3.7376E-02	1.1992E-02	4.4983E-03	3.8563E-03
	F10		F11		F12	
	AVG	STD	AVG	STD	AVG	STD
FATA	-1.2569E+04	2.6984E-04	-1.2498E+04	9.1213E+01	7.8917E+00	5.3959E+00
EPSO	-1.1440E+04	2.9627E+02	-2.3155E+03	4.3413E+02	5.9698E-01	1.0320E+00
ASCA_PSO	-7.1348E+03	9.1108E+02	0.0000E+00	0.0000E+00	3.3165E-02	1.8165E-01
SCADE	-1.2547E+04	1.2366E+02	1.3777E+02	2.0145E+01	3.3494E-02	1.8160E-01
SADE	-1.2554E+04	4.0950E+01	2.7050E+02	3.3882E+01	2.3869E-04	4.3208E-04
MPEDE	-1.1852E+04	2.8494E+02	0.0000E+00	0.0000E+00	1.3560E-14	3.6948E-15
LSHADE	-1.2716E+04	3.5841E+02	7.6280E-01	8.1308E-01	7.3243E+00	2.7768E-01
	F13		F14		F15	
	AVG	STD	AVG	STD	AVG	STD
FATA	8.8818E-16	0.0000E+00	8.5274E-03	1.0517E-02	1.5498E-03	4.1764E-03
EPSO	8.8381E-01	5.8693E-01	1.0014E+00	1.1883E-02	9.9622E-07	7.4340E-07
ASCA_PSO	1.6943E+00	1.0493E+00	0.0000E+00	0.0000E+00	4.6727E-13	2.5594E-12
SCADE	3.0699E+00	9.2455E-01	1.5685E-02	2.2234E-02	3.2847E+00	5.5332E-01
SADE	7.8752E-15	6.4863E-16	9.6795E-03	1.3175E-02	4.5153E-09	3.4356E-09
MPEDE	7.5199E-15	2.0298E-15	1.9227E-02	1.9609E-02	3.8011E-02	1.1053E-01

LSHADE	0.0000E+00	0.0000E+00	4.9241E-04	2.6971E-03	3.7799E-01	6.9633E-01
	F16		F17		F18	
	AVG	STD	AVG	STD	AVG	STD
FATA	2.8054E-01	4.4330E-01	7.3249E-04	2.7876E-03	1.9438E+07	1.1913E+07
EPSO	1.5705E-32	5.5674E-48	3.5346E-02	1.6312E-01	4.4866E+08	1.0608E+08
ASCA_PSO	1.1012E-01	2.6444E-01	2.5001E+00	8.9457E+00	5.1417E+05	3.0430E+05
SCADE	1.6675E-05	1.1884E-05	1.3498E-32	5.5674E-48	2.7407E+03	3.1824E+03
SADE	3.3661E-29	1.2827E-29	5.8742E-30	3.0440E-29	4.5651E+03	3.3472E+03
MPEDE	1.1748E+01	1.5730E+00	1.1239E+07	5.7214E+06	6.2950E+03	4.1368E+03
LSHADE	6.1631E-08	4.0652E-08	4.3766E+06	3.1628E+06	3.1151E+03	3.7619E+03
	F19		F20		F21	
	AVG	STD	AVG	STD	AVG	STD
FATA	9.2766E+07	4.4843E+07	2.0000E+02	9.1414E-15	8.0902E+02	6.4535E+00
EPSO	4.2271E+03	3.7318E+03	2.0000E+02	1.8283E-14	8.0182E+02	1.6543E+00
ASCA_PSO	8.1980E+08	1.6088E+09	8.8918E+02	1.5015E+01	8.0000E+02	7.8991E-14
SCADE	2.7901E+10	4.3551E+09	8.6718E+02	4.2872E+01	8.0099E+02	1.2256E+00
SADE	2.0000E+02	1.1212E-06	9.6542E+02	3.1291E+01	1.2019E+03	4.6235E-01
MPEDE	2.0000E+02	3.3225E-13	1.0732E+03	1.3717E+01	1.2022E+03	2.8892E-01
LSHADE	2.0000E+02	9.4346E-10	8.0136E+02	1.3446E+00	1.2024E+03	2.9903E-01
	F22		F23		F24	
	AVG	STD	AVG	STD	AVG	STD
FATA	1.2025E+03	2.4904E-01	1.4003E+03	5.1112E-02	1.4003E+03	5.4693E-02
EPSO	1.2007E+03	9.8278E-02	1.4036E+03	6.1571E+00	1.5801E+03	4.6584E+01
ASCA_PSO	1.2002E+03	1.0709E-01	1.4899E+03	1.3417E+01	1.5205E+03	1.2193E+00
SCADE	1.2001E+03	1.9299E-02	1.4002E+03	4.5782E-02	1.5218E+03	8.1653E+00
SADE	1.2001E+03	4.5433E-02	1.4003E+03	1.1098E-01	2.0155E+04	8.1817E+03
MPEDE	1.2002E+03	2.9181E-02	1.4003E+03	1.9590E-01	1.5066E+03	2.5696E+00
LSHADE	1.4004E+03	3.0883E-01	1.4002E+03	5.1687E-02	1.5065E+03	2.5125E+00
	F25		F26		F27	
	AVG	STD	AVG	STD	AVG	STD
FATA	1.5079E+03	3.4419E+00	3.9606E+04	2.5935E+04	3.4932E+06	1.0186E+06
EPSO	1.5042E+03	8.9486E-01	3.8917E+03	2.1553E+03	1.9035E+08	1.0822E+08
ASCA_PSO	1.5045E+03	1.8969E+00	3.4802E+03	5.1461E+02	2.6969E+03	1.0934E+03
SCADE	5.5438E+05	2.7812E+05	2.6859E+03	3.8436E+02	1.9343E+03	6.3777E+01
SADE	2.8966E+05	1.7388E+05	7.5859E+03	6.5591E+03	1.9407E+03	5.3221E+01
MPEDE	1.0918E+06	9.2421E+05	1.0658E+04	5.4507E+03	1.8671E+03	2.6858E+01
LSHADE	1.5142E+07	6.4375E+06	3.8845E+03	1.9615E+03	1.9201E+03	4.8875E+01
	F28		F29		F30	
	AVG	STD	AVG	STD	AVG	STD
FATA	5.0551E+03	3.5146E+03	2.0443E+03	1.9956E+01	2.9931E+03	2.5688E+02
EPSO	2.4889E+03	1.7840E+02	2.2439E+03	1.0793E+02	3.2282E+03	3.4756E+02
ASCA_PSO	6.5790E+03	3.0319E+03	2.5295E+05	2.2337E+05	2.4179E+03	1.4270E+02
SCADE	2.6725E+04	1.0972E+04	8.4055E+04	7.0011E+04	3.3348E+03	4.3646E+02
SADE	2.9092E+03	1.0155E+03	3.1517E+05	2.3189E+05	2.5000E+03	1.8882E-13

MPEDE	2.1438E+03	8.0688E+01	2.0861E+06	8.2451E+05	2.6152E+03	1.5866E-12
LSHADE	2.2773E+03	9.9160E+01	2.5035E+04	2.3401E+04	2.6244E+03	6.4375E+00

Table. A.11 The results of FATA with SOTAs

	Item	FATA	RIME	HHO	LCA	XMACO
F1	AVG	0.000000E+00	1.540159E-03	0.000000E+00	5.178397E-02	8.784313E-65
	STD	0.000000E+00	6.121798E-04	0.000000E+00	1.219728E-01	2.192107E-64
F2	AVG	0.000000E+00	2.284052E-02	0.000000E+00	6.805392E-02	1.809511E-42
	STD	0.000000E+00	5.750768E-03	0.000000E+00	4.455237E-02	3.621170E-42
F3	AVG	0.000000E+00	1.720765E+00	0.000000E+00	1.165992E+01	3.527705E-02
	STD	0.000000E+00	5.514127E-01	0.000000E+00	1.677904E+01	1.701402E-01
F4	AVG	0.000000E+00	1.312815E-01	0.000000E+00	3.109849E-02	9.229357E+00
	STD	0.000000E+00	4.011424E-02	0.000000E+00	2.208257E-02	2.496022E+00
F5	AVG	3.370509E-02	1.535941E+02	5.297389E-05	3.631924E-01	3.171710E+01
	STD	4.913610E-02	1.742931E+02	6.300986E-05	4.367464E-01	3.297018E+01
F6	AVG	1.695415E-04	1.365396E-03	7.699031E-07	4.124757E-02	9.260898E-30
	STD	1.598213E-04	4.287466E-04	1.040030E-06	5.975909E-02	1.232617E-29
F7	AVG	3.241013E-06	2.744184E-03	9.168102E-06	4.473608E-06	7.867521E-03
	STD	3.123532E-06	8.685897E-04	6.470826E-06	4.798588E-06	3.637019E-03
F8	AVG	-1.256949E+04	-1.182352E+04	-1.256948E+04	-9.14983E+03	-8.033974E+03
	STD	2.017907E-04	2.768111E+02	4.141662E-03	4.358316E+03	1.029616E+03
F9	AVG	0.000000E+00	1.038158E+01	0.000000E+00	2.368259E+01	1.336208E+02
	STD	0.000000E+00	3.099183E+00	0.000000E+00	7.258969E+01	2.474358E+01
F10	AVG	8.881784E-16	9.907955E-03	8.881784E-16	3.308414E-02	1.952424E-01
	STD	0.000000E+00	2.384360E-03	0.000000E+00	2.296427E-02	5.202887E-01
F11	AVG	0.000000E+00	1.685198E-02	0.000000E+00	6.191897E-02	1.319884E-02
	STD	0.000000E+00	1.245912E-02	0.000000E+00	8.092154E-02	1.280210E-02
F12	AVG	1.021118E-06	5.369389E-06	6.255889E-08	2.002876E-04	1.244951E-01
	STD	7.046309E-07	2.440070E-06	1.001547E-07	2.663002E-04	2.576382E-01
F13	AVG	1.467991E-05	1.174860E-03	4.184567E-07	2.267203E-03	1.652346E-01
	STD	1.388390E-05	3.354973E-03	6.426535E-07	3.471358E-03	4.918578E-01
F14	AVG	1.285229E+07	3.486703E+06	1.120045E+07	1.771880E+09	5.283618E+05
	STD	4.808827E+06	1.200219E+06	5.471588E+06	2.101731E+08	4.825369E+05
F15	AVG	8.208299E+07	1.358916E+04	1.156701E+07	8.898099E+10	1.460839E+04
	STD	4.072217E+07	1.235849E+04	2.077717E+06	6.883579E+09	1.216563E+04
F16	AVG	8.948514E+02	8.102489E+02	9.043966E+02	1.183016E+03	9.259211E+02
	STD	1.268418E+01	2.508181E+00	1.971930E+01	1.720506E+01	4.020150E+01
F17	AVG	1.201569E+03	1.200256E+03	1.201527E+03	1.204725E+03	1.202424E+03
	STD	4.886636E-01	1.097107E-01	3.897588E-01	7.192661E-01	2.673691E-01
F18	AVG	1.400466E+03	1.400377E+03	1.400279E+03	1.669137E+03	1.400318E+03
	STD	3.209822E-01	1.883237E-01	5.089668E-02	3.140403E+01	1.269725E-01
F19	AVG	1.584530E+03	1.506877E+03	1.538252E+03	2.149790E+05	1.515974E+03

	STD	5.190484E+01	1.589687E+00	6.865304E+00	6.358433E+04	2.048185E+00
F20	AVG	6.373234E+05	3.283718E+05	1.372888E+06	2.489311E+08	9.627220E+04
	STD	5.754200E+05	2.356570E+05	7.527834E+05	1.058694E+08	8.282974E+04
F21	AVG	1.730563E+04	5.531229E+03	1.178553E+05	8.979664E+09	3.801500E+03
	STD	5.095039E+04	5.815448E+03	1.254844E+05	2.486085E+09	2.417629E+03
F22	AVG	5.176854E+03	2.084004E+03	1.295581E+04	4.546782E+06	3.271375E+03
	STD	4.296875E+03	2.058765E+01	6.521020E+03	4.830186E+06	1.488468E+03
F23	AVG	2.408563E+05	9.653402E+04	4.489129E+05	2.233873E+08	9.040250E+04
	STD	2.155799E+05	8.805709E+04	4.288032E+05	1.582875E+08	8.621936E+04
F24	AVG	2.500000E+03	2.615251E+03	2.500000E+03	2.623097E+03	2.615244E+03
	STD	0.000000E+00	4.026581E-03	0.000000E+00	2.771489E+02	3.878934E-12
F25	AVG	2.600000E+03	2.630244E+03	2.600000E+03	2.601118E+03	2.623828E+03
	STD	2.308399E-07	6.261961E+00	2.196887E-04	6.133776E-01	4.303813E+00
F26	AVG	2.700000E+03	2.707996E+03	2.700000E+03	2.700045E+03	2.704351E+03
	STD	0.000000E+00	2.622962E+00	0.000000E+00	3.833341E-02	1.194956E+00
F27	AVG	2.900003E+03	3.282220E+03	2.900000E+03	4.774044E+03	3.109764E+03
	STD	5.431682E-03	1.475035E+02	0.000000E+00	3.310412E+02	5.271396E+01
F28	AVG	3.000000E+03	3.759825E+03	3.000000E+03	1.028040E+04	3.751301E+03
	STD	0.000000E+00	1.275049E+02	0.000000E+00	2.592957E+03	1.172257E+02
F29	AVG	3.100000E+03	4.658623E+03	4.862847E+03	1.153858E+08	7.505751E+05
	STD	0.000000E+00	6.088450E+02	5.679746E+03	2.379547E+08	2.298282E+06
F30	AVG	3.200000E+03	6.806411E+03	8.254552E+03	1.421954E+07	7.946084E+03
	STD	0.000000E+00	1.235544E+03	1.433031E+04	6.973939E+06	5.636014E+03

Table. A.12 The computational cost of this experiment

	FATA	MVO	SCA	AOA	GSA
F1	47.266	58.594	35.781	1074.266	228.063
F2	48.594	57.188	36.953	1115.500	227.234
F3	127.734	132.859	114.625	3479.781	305.516
F4	45.578	58.359	35.313	1084.828	225.391
F5	56.031	65.969	43.797	1342.016	234.797
F6	47.938	58.281	35.500	1093.250	226.719
F7	81.156	90.438	68.281	2069.578	263.031
F8	56.078	49.719	45.172	1388.031	238.125
F9	49.938	65.250	39.359	1154.172	235.266
F10	51.438	66.656	43.344	1194.906	236.453
F11	56.938	73.516	47.156	1402.688	240.875
F12	144.422	151.625	132.125	3965.984	329.281
F13	146.875	156.625	133.938	3841.594	336.797
F14	72.219	81.984	59.797	1675.125	260.516
F15	65.313	77.047	53.016	1469.719	254.297
F16	64.125	77.688	53.672	1447.719	252.953
F17	143.625	158.000	133.438	3881.891	334.563

F18	65.797	77.781	53.344	1477.781	254.563
F19	70.016	79.609	58.516	1643.281	258.531
F20	75.859	82.703	64.000	1720.422	263.453
F21	68.641	79.563	56.688	1536.313	257.281
F22	69.719	75.031	58.234	1589.500	258.672
F23	73.281	80.016	61.531	1680.547	262.266
F24	137.891	151.188	129.547	3707.672	327.281
F25	116.750	134.125	107.359	2979.203	308.453
F26	126.578	144.328	123.516	3333.422	319.266
F27	595.609	598.234	589.563	17188.906	767.047
F28	166.484	180.734	160.641	4454.625	352.203
F29	193.500	219.859	200.938	5744.734	392.547
F30	128.531	137.547	120.938	3426.969	314.969
	DE	ACOR	PSO	WOA	CSA
F1	121.906	168.313	18.875	17.047	20.703
F2	124.250	169.703	19.969	18.406	22.406
F3	194.219	248.469	97.922	96.391	100.063
F4	115.906	168.297	19.047	16.797	20.672
F5	126.172	177.172	27.250	25.297	29.563
F6	115.828	169.125	19.063	16.922	20.734
F7	148.328	202.750	51.359	49.672	53.469
F8	125.500	179.281	29.297	25.094	29.516
F9	118.969	175.266	25.781	18.813	25.672
F10	119.563	173.953	26.703	19.703	27.609
F11	128.672	181.344	32.094	26.656	33.375
F12	220.781	271.469	116.078	112.172	116.547
F13	221.609	274.672	118.234	113.406	118.406
F14	146.578	201.234	42.688	40.266	43.891
F15	142.063	194.797	35.734	33.344	37.359
F16	137.609	192.094	35.797	32.609	36.531
F17	220.016	275.031	116.516	113.609	117.719
F18	140.438	194.672	36.172	33.703	37.531
F19	144.219	198.688	40.203	37.891	41.500
F20	152.719	204.234	45.484	43.047	46.703
F21	145.094	197.422	38.844	36.359	40.109
F22	146.109	199.688	40.516	37.703	41.438
F23	150.563	202.672	43.906	41.313	44.984
F24	215.188	267.172	108.688	106.484	110.813
F25	194.906	246.578	91.938	84.172	91.313
F26	213.328	256.859	102.578	96.875	101.875
F27	671.766	669.563	559.688	561.969	568.547
F28	247.563	291.172	136.641	135.438	137.875
F29	286.922	326.781	181.875	171.172	177.719
F30	206.656	254.813	99.672	96.750	100.672

Table. A.13 The computational cost of FATA with SOTAs

	FATA	RIME	HHO	LCA	XMACO
F1	48.469	38.938	31.953	438.203	247.016
F2	49.781	38.688	32.438	473.828	247.953
F3	114.094	103.734	108.688	2415.656	319.703
F4	45.281	37.594	30.063	443.000	252.281
F5	54.406	44.641	39.391	656.141	259.719
F6	47.281	37.375	30.750	448.109	237.281
F7	78.547	68.422	66.516	1367.031	281.484
F8	55.641	44.797	40.047	673.141	249.563
F9	49.797	41.859	34.141	587.734	259.266
F10	51.656	43.547	35.859	646.172	253.078
F11	56.625	49.609	42.203	808.656	263.594
F12	137.531	128.031	134.953	3125.750	336.250
F13	138.016	128.344	135.109	3142.500	339.969
F14	68.453	59.250	55.578	1064.734	276.344
F15	60.938	52.453	48.047	872.672	269.594
F16	60.703	51.672	46.813	823.266	271.766
F17	137.984	129.391	138.078	3155.938	348.500
F18	62.203	52.750	48.438	876.906	271.813
F19	67.000	56.531	52.609	953.734	272.578
F20	71.734	62.063	58.781	1117.438	278.750
F21	64.641	55.469	51.281	941.547	273.344
F22	66.328	56.797	52.719	961.766	274.344
F23	69.844	60.281	56.797	1083.438	278.375
F24	131.688	122.156	128.781	2933.656	338.594
F25	112.219	104.781	104.703	2345.547	321.063
F26	122.359	115.641	117.672	2651.219	331.500
F27	574.094	550.453	600.734	16091.484	759.906
F28	160.156	149.750	150.297	3628.781	363.250
F29	190.609	189.109	192.531	4841.844	403.984
F30	124.313	114.078	117.313	2608.188	325.875

Table. A.14 The computational cost of FATA with SOTAs

	FATA	ACWOA	m_SCA	HGW0	CGSCA	AMFOA	DSMFO	SFOA
F1	48.469	21.672	37.672	94.813	98.609	27.047	74.734	19.172
F2	49.781	22.688	38.469	96.594	100.438	27.984	76.313	20.625
F3	114.094	90.125	109.484	161.578	167.516	91.734	143.391	85.453
F4	45.281	21.906	37.266	95.328	99.297	26.172	73.719	19.453
F5	54.406	28.063	44.672	102.438	106.313	33.141	83.531	25.953
F6	47.281	21.156	37.188	95.250	99.328	26.391	76.203	19.406
F7	78.547	52.094	71.031	126.031	130.688	56.531	97.469	49.734
F8	55.641	29.234	47.234	102.266	108.969	33.891	85.281	25.828
F9	49.797	22.547	40.375	96.688	101.297	27.766	74.500	21.141
F10	51.656	23.516	45.641	97.781	102.484	28.938	75.453	22.281

F11	56.625	29.422	48.031	104.672	108.516	34.828	81.813	28.125
F12	137.531	110.516	135.797	184.672	189.906	115.391	167.750	108.016
F13	138.016	112.016	135.734	183.922	189.438	115.844	168.156	108.813
F14	68.453	41.844	59.922	116.375	120.531	46.766	98.156	39.563
F15	60.938	35.313	52.891	110.391	114.172	40.250	92.000	33.063
F16	60.703	34.844	52.906	109.109	115.125	38.594	90.828	31.313
F17	137.984	112.828	136.922	187.125	191.594	119.219	170.656	110.859
F18	62.203	35.594	52.859	110.234	114.266	40.234	91.734	33.094
F19	67.000	39.734	58.031	114.266	119.281	44.750	95.906	37.484
F20	71.734	44.813	63.672	118.078	125.141	48.469	101.734	41.063
F21	64.641	38.547	56.203	112.516	118.125	42.484	95.203	35.313
F22	66.328	39.781	57.594	113.453	119.266	43.828	96.344	36.625
F23	69.844	43.563	61.719	116.578	123.000	47.281	100.141	39.781
F24	131.688	104.234	130.281	178.453	183.422	108.828	156.109	101.234
F25	112.219	82.391	107.734	156.266	162.125	87.297	134.281	79.500
F26	122.359	93.438	124.297	167.188	173.484	98.188	145.781	90.531
F27	574.094	543.859	615.797	597.438	566.422	489.969	532.656	481.578
F28	160.156	124.484	162.875	207.281	200.328	124.531	172.844	116.750
F29	190.609	170.703	204.984	235.031	232.609	156.750	203.250	149.000
F30	124.313	97.734	122.484	168.531	171.969	95.734	142.891	88.094

Reference

1. Cao, B., et al., *Multiobjective 3-D Topology Optimization of Next-Generation Wireless Data Center Network*. IEEE Transactions on Industrial Informatics, 2019. **16**(5): p. 3597-3605.
2. Cao, B., et al., *Applying graph-based differential grouping for multiobjective large-scale optimization*. Swarm and Evolutionary Computation, 2020. **53**: p. 100626.
3. Lu, C., et al., *Human–Robot Collaborative Scheduling in Energy-Efficient Welding Shop*. IEEE Transactions on Industrial Informatics, 2024. **20**(1): p. 963-971.
4. Xie, Y., et al., *A Two-Stage Estimation of Distribution Algorithm With Heuristics for Energy-Aware Cloud Workflow Scheduling*. IEEE Transactions on Services Computing, 2023. **16**(6): p. 4183-4197.
5. Yu, F., et al., *A knowledge-guided bi-population evolutionary algorithm for energy-efficient scheduling of distributed flexible job shop problem*. Engineering Applications of Artificial Intelligence, 2024. **128**: p. 107458.
6. Cao, B., et al., *Diversified personalized recommendation optimization based on mobile data*. IEEE Transactions on Intelligent Transportation Systems, 2020. **22**(4): p. 2133-2139.
7. Liu, H., L. Cai, and T. Zou, *Gradient descent based self-adaptive step length estimation method, involves performing gradient descent algorithm iteration process, and estimating position of person by utilizing track estimation algorithm*. UNIV SOUTHEAST (UYSE-C) UNIV SOUTHEAST WUXI INTEGRATED CIRCUIT (UYSE-C) NANJING SAMPLE TECHNOLOGY CO LTD (NANJ-Non-standard).
8. Liu, Z., et al., *Application of a novel EWMA-phi chart on quality control in asphalt mixtures production*. Construction and Building Materials, 2022. **323**.

9. Han, T. and Z. Wang, *CNN model based rolling bearing fault diagnosis method, involves defining regularization parameter learning rate decay function, and determining whether CNN model meets accuracy requirement based on decay function*. Univ Beijing Sci & Technology (Unbs-C).
10. Tu, J.Z., et al., *Evolutionary biogeography-based whale optimization methods with communication structure: Towards measuring the balance*. Knowledge-Based Systems, 2021. **212**: p. 31.
11. Dai, M., et al., *PSACCF: Prioritized online slice admission control considering fairness in 5G/B5G networks*. IEEE Transactions on Network Science and Engineering, 2022. **9**(6): p. 4101-4114.
12. Liang, J., B. Qu, and P. Suganthan, *Problem definitions and evaluation criteria for the CEC 2014 special session and competition on single objective real-parameter numerical optimization*, ed. CEC2014. 2013.
13. Lu, C., et al., *A Pareto-based hybrid iterated greedy algorithm for energy-efficient scheduling of distributed hybrid flowshop*. Expert Systems with Applications, 2022. **204**: p. 117555.
14. Socha, K. and M. Dorigo, *Ant colony optimization for continuous domains*. European Journal of Operational Research, 2008. **185**(3): p. 1155-1173.
15. Kennedy, J. and R. Eberhart. *Particle swarm optimization*. in *Proceedings of ICNN'95 - International Conference on Neural Networks*. 1995.
16. Cao, B., et al., *RFID Reader Anticollision Based on Distributed Parallel Particle Swarm Optimization*. IEEE Internet of Things Journal, 2021. **8**(5): p. 3099-3107.
17. Lynn, N. and P.N. Suganthan, *Ensemble particle swarm optimizer*. Applied Soft Computing, 2017. **55**: p. 533-548.
18. Issa, M., et al., *ASCA-PSO: Adaptive sine cosine optimization algorithm integrated with particle swarm for pairwise local sequence alignment*. Expert Systems with Applications, 2018. **99**: p. 56-70.
19. Mirjalili, S., *Moth-flame optimization algorithm: A novel nature-inspired heuristic paradigm*. Knowledge-based systems, 2015. **89**: p. 228-249.
20. Chen, C.C., et al., *Soil Erosion Prediction Based on Moth-Flame Optimizer-Evolved Kernel Extreme Learning Machine*. Electronics, 2021. **10**(17).
21. Li, S., et al., *Slime mould algorithm: A new method for stochastic optimization*. Future Generation Computer Systems, 2020.
22. Heidari, A.A., et al., *Harris hawks optimization: Algorithm and applications*. Future Generation Computer Systems, 2019. **97**: p. 849-872.
23. Askarzadeh, A., *A novel metaheuristic method for solving constrained engineering optimization problems: Crow search algorithm*. Computers & Structures, 2016. **169**: p. 1-12.
24. Yang, X.-S., *A new metaheuristic bat-inspired algorithm*, in *Nature inspired cooperative strategies for optimization (NICSO 2010)*. 2010, Springer. p. 65-74.
25. Tu, J., et al., *The Colony Predation Algorithm*. Journal of Bionic Engineering, 2021. **18**(3): p. 674-710.
26. Yang, Y., et al., *Hunger games search: Visions, conception, implementation, deep analysis, perspectives, and towards performance shifts*. Expert Systems with Applications, 2021. **177**: p. 114864.
27. Lian, J., et al., *Parrot optimizer: Algorithm and applications to medical problems*. Computers in Biology and Medicine, 2024: p. 108064.
28. Houssein, E.H., et al., *Liver Cancer Algorithm: A novel bio-inspired optimizer*. Computers in Biology and Medicine, 2023. **165**: p. 107389.
29. Yang, X.-S. *Firefly Algorithms for Multimodal Optimization*. 2009. Berlin, Heidelberg: Springer Berlin Heidelberg.
30. Mirjalili, S., S.M. Mirjalili, and A. Lewis, *Grey Wolf Optimizer*. Advances in Engineering Software, 2014. **69**: p. 46-61.

31. Mirjalili, S. and A. Lewis, *The Whale Optimization Algorithm*. Advances in Engineering Software, 2016. **95**: p. 51-67.
32. Pan, W.T., *A new Fruit Fly Optimization Algorithm: Taking the financial distress model as an example*. Knowledge-Based Systems, 2012. **26**: p. 69-74.
33. Yin, L., et al., *Energy saving in flow-shop scheduling management: an improved multiobjective model based on grey wolf optimization algorithm*. Mathematical Problems in Engineering, 2020. **2020**: p. 1-14.
34. Zhu, A., et al., *Hybridizing grey wolf optimization with differential evolution for global optimization and test scheduling for 3D stacked SoC*. Journal of Systems Engineering and Electronics, 2015. **26**(2): p. 317-328.
35. Elhosseini, M.A., et al., *Biped robot stability based on an A-C parametric Whale Optimization Algorithm*. Journal of Computational Science, 2019. **31**: p. 17-32.
36. Li, H., et al., *SMWO/D: a decomposition-based switching multi-objective whale optimiser for structural optimisation of Turbine disk in aero-engines*. International Journal of Systems Science, 2023. **54**(8): p. 1713-1728.
37. Wang, W.C. and X.G. Liu, *Melt index prediction by least squares support vector machines with an adaptive mutation fruit fly optimization algorithm*. Chemometrics and Intelligent Laboratory Systems, 2015. **141**: p. 79-87.
38. Hu, R., et al., *A short-term power load forecasting model based on the generalized regression neural network with decreasing step fruit fly optimization algorithm*. Neurocomputing, 2017. **221**: p. 24-31.
39. Storn, R. and K.J.J.o.G.O. Price, *Differential Evolution – A Simple and Efficient Heuristic for global Optimization over Continuous Spaces*. 1997. **11**(4): p. 341-359.
40. Qin, A.K., V.L. Huang, and P.N. Suganthan, *Differential Evolution Algorithm With Strategy Adaptation for Global Numerical Optimization*. Ieee Transactions on Evolutionary Computation, 2009. **13**(2): p. 398-417.
41. Sastry, K., D.E. Goldberg, and G. Kendall, *Genetic Algorithms*, in *Search Methodologies*. 2014. p. 93-117.
42. Mou, J., et al., *A Machine Learning Approach for Energy-Efficient Intelligent Transportation Scheduling Problem in a Real-World Dynamic Circumstances*. IEEE Transactions on Intelligent Transportation Systems, 2023. **24**(12): p. 15527-15539.
43. Li, H., et al., *A Novel Dynamic Multiobjective Optimization Algorithm With Non-Inductive Transfer Learning Based on Multi-Strategy Adaptive Selection*. Ieee Transactions on Neural Networks and Learning Systems, 2023.
44. Li, H., et al., *A Novel Dynamic Multiobjective Optimization Algorithm With Hierarchical Response System*. Ieee Transactions on Computational Social Systems, 2023.
45. Rao, R.V., V.J. Savsani, and D.P. Vakharia, *Teaching-Learning-Based Optimization: An optimization method for continuous non-linear large scale problems*. Information Sciences, 2012. **183**(1): p. 1-15.
46. David, B.F., *Artificial Intelligence through Simulated Evolution*, in *Evolutionary Computation: The Fossil Record*. 1998, IEEE. p. 227-296.
47. Ahmadianfar, I., et al., *INFO: An Efficient Optimization Algorithm based on Weighted Mean of Vectors*. Expert Systems with Applications, 2022: p. 116516.
48. Ahmadianfar, I., et al., *RUN Beyond the Metaphor: An Efficient Optimization Algorithm Based on Runge Kutta Method*. Expert Systems with Applications, 2021: p. 115079.
49. Sun, G., et al., *Low-latency and resource-efficient service function chaining orchestration in network function virtualization*. IEEE Internet of Things Journal, 2019. **7**(7): p. 5760-5772.

50. Mirjalili, S., S.M. Mirjalili, and A. Hatamlou, *Multi-Verse Optimizer: a nature-inspired algorithm for global optimization*. Neural Computing & Applications, 2016. **27**(2): p. 495-513.
51. Rashedi, E., H. Nezamabadi-Pour, and S. Saryazdi, *GSA: a gravitational search algorithm*. Information sciences, 2009. **179**(13): p. 2232-2248.
52. Shah-Hosseini, H. and Ieee. *Problem solving by intelligent water drops*. in *IEEE Congress on Evolutionary Computation*. 2007. Singapore, SINGAPORE.
53. Mirjalili, S., *SCA: a sine cosine algorithm for solving optimization problems*. Knowledge-based systems, 2016. **96**: p. 120-133.
54. Kumar, N., et al., *Single Sensor-Based MPPT of Partially Shaded PV System for Battery Charging by Using Cauchy and Gaussian Sine Cosine Optimization*. Ieee Transactions on Energy Conversion, 2017. **32**(3): p. 983-992.
55. Chen, D.B., et al., *Poplar optimization algorithm: A new meta-heuristic optimization technique for numerical optimization and image segmentation*. Expert Systems with Applications, 2022. **200**.
56. Blanco-García, J., J. Vázquez Dorrió, and F. Ribas, *PHOTOGRAPHING MIRAGES ABOVE THE SEA SURFACE*. 2011.
57. Garcia, S., et al., *Advanced nonparametric tests for multiple comparisons in the design of experiments in computational intelligence and data mining: Experimental analysis of power*. Information Sciences, 2010. **180**(10): p. 2044-2064.
58. Derrac, J., et al., *A practical tutorial on the use of nonparametric statistical tests as a methodology for comparing evolutionary and swarm intelligence algorithms*. Swarm and Evolutionary Computation, 2011. **1**(1): p. 3-18.
59. Abualigah, L., et al., *The Arithmetic Optimization Algorithm*. Computer Methods in Applied Mechanics and Engineering, 2021. **376**: p. 113609.
60. Qu, C., et al., *A Modified Sine-Cosine Algorithm Based on Neighborhood Search and Greedy Levy Mutation*. Computational intelligence and neuroscience, 2018. **2018**: p. 4231647-4231647.
61. Nenavath, H. and R.K. Jatoth, *Hybridizing sine cosine algorithm with differential evolution for global optimization and object tracking*. Applied Soft Computing, 2018. **62**: p. 1019-1043.
62. Wu, G.H., et al., *Differential evolution with multi-population based ensemble of mutation strategies*. Information Sciences, 2016. **329**: p. 329-345.
63. Su, H., et al., *RIME: A physics-based optimization*. Neurocomputing, 2023.
64. Heidari, A.A., et al., *Harris hawks optimization: Algorithm and applications*. Future Generation Computer Systems-the International Journal of Escience, 2019. **97**: p. 849-872.
65. Qi, A., et al., *Directional mutation and crossover boosted ant colony optimization with application to COVID-19 X-ray image segmentation*. Comput Biol Med, 2022. **148**: p. 105810.
66. Liang, J.J., B.Y. Qu, and P.N. Suganthan, *Problem definitions and evaluation criteria for the CEC 2014 special session and competition on single objective real-parameter numerical optimization*. Computational Intelligence Laboratory, Zhengzhou University, Zhengzhou China and Technical Report, Nanyang Technological University, Singapore, 2013. **635**(2): p. 2014.
67. Xu, X. and Z. Wei, *Dynamic pickup and delivery problem with transshipments and LIFO constraints*. Computers & Industrial Engineering, 2023. **175**: p. 108835.
68. Zhao, T., et al., *A comprehensive review of process planning and trajectory optimization in arc-based directed energy deposition*. Journal of Manufacturing Processes, 2024. **119**: p. 235-254.
69. Eskandar, H., et al., *Water cycle algorithm – A novel metaheuristic optimization method for solving constrained engineering optimization problems*. Computers & Structures, 2012. **110-111**: p. 151-166.

70. Mahdavi, M., M. Fesanghary, and E. Damangir, *An improved harmony search algorithm for solving optimization problems*. Applied Mathematics and Computation, 2007. **188**(2): p. 1567-1579.
71. Huang, F.-z., L. Wang, and Q. He, *An effective co-evolutionary differential evolution for constrained optimization*. Applied Mathematics and Computation, 2007. **186**(1): p. 340-356.
72. Wagdy, A., *A novel differential evolution algorithm for solving constrained engineering optimization problems*. Journal of Intelligent Manufacturing, 2017.
73. Wang, G.C., et al., *Chaotic Arc Adaptive Grasshopper Optimization*. Ieee Access, 2021. **9**: p. 17672-17706.
74. Coello Coello, C.A., *Use of a self-adaptive penalty approach for engineering optimization problems*. Computers in Industry, 2000. **41**(2): p. 113-127.
75. He, Q. and L. Wang, *An effective co-evolutionary particle swarm optimization for constrained engineering design problems*. Vol. 20. 2007. 89-99.
76. Sandgren, E., *Nonlinear integer and discrete programming in mechanical design*. Vol. 14. 1988.
77. Li, S.M., et al., *Slime mould algorithm: A new method for stochastic optimization*. Future Generation Computer Systems-the International Journal of Escience, 2020. **111**: p. 300-323.
78. Cheng, M.-Y. and D. Prayogo, *Symbiotic Organisms Search: A new metaheuristic optimization algorithm*. Vol. 139. 2014.
79. Chickermane, H. and H.C. Gea, *Structural optimization using a new local approximation method*. International Journal for Numerical Methods in Engineering, 1996. **39**(5): p. 829-846.
80. Gandomi, A., X.-S. Yang, and A. Alavi, *Cuckoo search algorithm: a metaheuristic approach to solve structural optimization problems*. Vol. 29. 2013. 1-19.